*Geochimica et Cosmochimica Acta* Vol. 53, pp. 1307–1322

0016-7037/89/$3.00 + .00

# Irradiation of organic matter by uranium decay in the Alum Shale, Sweden

M. D. LEWAN[1] and B. BUCHARDT[2]

[1]Amoco Production Company, Research Center, P.O. Box 3385, Tulsa, OK 74102, U.S.A.
[2]University of Copenhagen, Department of Geology, Øster Voldgade 10, DK-1350 Copenhagen K, Denmark

(*Received May* 27, 1988; *accepted in revised form March* 13, 1989)

**Abstract**—The Alum Shale of Sweden contains black shales with anomalously high uranium concentrations in excess of 100 ppm. Syngenetic or early diagenetic origin of this uranium indicates that organic matter within these shales has been irradiated by decaying uranium for approximately 500 Ma. Radiation-induced polymerization of alkanes through a free-radical cross-linking mechanism appears to be responsible for major alterations within the irradiated organic matter. Specific radiation-induced alterations include generation of condensate-like oils at reduced yields from hydrous pyrolysis experiments, decrease in atomic H/C ratios of kerogens, decrease in bitumen/organic-carbon ratios, and a relative increase in low-molecular weight triaromatic steroid hydrocarbons. Conversely, stable carbon isotopes of kerogens, reflectance of vitrinite-like macerals, oil-generation kinetics, and isomerization of 20R to 20S $\alpha\alpha$ $C_{29}$-steranes were not affected by radiation. The radiation dosage needed to cause the alterations observed in the Alum Shale has been estimated to be in excess of $10^5$ Mrads with respect to organic carbon. This value is used to estimate the potential for radiation damage to thermally immature organic matter in black shales through the geological rock record. High potential for radiation damage is not likely in Cenozoic and Mesozoic black shales but becomes more likely in lower Paleozoic and Precambrian black shales.

## INTRODUCTION

SYNGENETIC OR EARLY diagenetic enrichment of uranium in black shales is a common geochemical phenomenon. Shales overall have average uranium contents between 3 and 7 ppm (TUREKIAN and WEDEPOHL, 1961; RONOV and MIGDISOV, 1971), while black shales have average uranium contents ranging from 3 to 1244 ppm (BATES and STRAHL, 1958). This enrichment is generally attributed to the ability of organic matter to extract uranium from solution and to slow sedimentation that allows ample time for removal of dissolved uranium from interstitial waters. SWANSON (1960, 1961) advocates organic matter derived from vascular land plants as an important constituent for concentrating uranium. Conversely, BREGER and BROWN (1963), OLSON (1982), and DEGENS *et al.* (1977) report no relationship between uranium and organic matter derived from vascular land plants in the Chattanooga Shale, Woodford Shale, and Black Sea sediments, respectively. Association of uranium with black shales and irradiation experiments with fatty acids prompted SHEPPARD (1944) to consider petroleum generation a result of natural radioactivity. Although the amount of petroleum generated in this manner has been shown to be insignificant (WHITEHEAD, 1954), radiation damage to organic matter in contact with uranium has been documented (*e.g.*, PIERCE *et al.*, 1958). The majority of studies showing radiation damage to organic matter involve coals (TEICHMÜLLER and TEICHMÜLLER, 1958; JEDWAB, 1966), coalified logs (ERGUN *et al.*, 1960; BREGER, 1974; GENTRY *et al.*, 1976; SASSEN, 1983), and sedimentary wood debris (HATCHER *et al.*, 1986) in contact with epigenetic uranium minerals.

Anomalously high concentrations of uranium in the Alum Shale of Scandinavia offers an ideal situation for further evaluation of natural irradiation effects on oil-prone organic matter. This Lower Ordovician to Middle Cambrian black shale typically has organic carbon contents ranging from 5 to 20 weight percent and was retorted for oil in Sweden from 1923 to 1969 (ARMANDS, 1972). Uranium concentrations usually range from 50 to 200 ppm, but in central Sweden concentrations of 200 to more than 400 ppm are common within the *Peltura scarabaeoides* zone of the Upper Cambrian (ANDERSSON *et al.*, 1983, 1985). Organic lenses referred to as kolm occur sporadically within this zone and have uranium concentrations as high as 7000 ppm (BATES *et al.*, 1956). HOERING and NAVALE (1987) suggested that radiation damage from decaying uranium may be responsible for the lack of biological markers within kolm lenses. The syngenetic or early diagenetic enrichment of uranium in the Alum Shale indicates its organic matter has been exposed to radiation from decaying uranium for approximately 500 Ma. Evaluating the effects of this radiation on the organic matter in thermally immature samples of Alum Shale having a broad range of uranium concentrations is the objective of this study.

Thermal stress experienced by the Alum Shale ranges from thermal immaturity in outliers of central Sweden (BUCHARDT *et al.*, 1986) to low-grade metamorphism in the Oslo Graben (BRYHNI and BRASTAD, 1980). In order to avoid confusing variations in thermal stress within radiation effects, only thermally immature samples of the Alum Shale were considered. Thermal immaturity is used here to describe rocks that have not undergone petroleum generation and expulsion through the thermal decomposition of their kerogens. A useful index of thermal stress experienced by the Alum Shale was found to be the mean reflectance of vitrinite-like macerals in polished kerogen slides (BUCHARDT and LEWAN, 1989). Although lack of vascular land plants in pre-Silurian rocks (BANKS, 1975) excludes the presence of true vitrinite, reflectance of vitrinite-like macerals in pre-Silurian rocks has been shown to be useful in indexing thermal maturity levels (SIKANDER and PITTON, 1978; KISCH, 1980). Similar to vitrinite reflectance measurements in post-Silurian rocks, reflectance values less than 0.54% $R_0$ for vitrinite-like macerals in the Alum Shale are indicative of thermal immaturity.

## METHODS

*Sample collection:* Thermally immature samples of Alum Shale with uranium concentrations from 18 to 440 ppm were collected from quarries and cores in outliers of central Sweden, coastal outcrops on Öland, and a core from a well in the Baltic Sea. Outlier plateaus in Västergötland are capped by a Permo-Carboniferous diabase intrusion (PRIEM *et al.*, 1968), which had an original thickness of approximately 60 meters. This tabular intrusion is discordant with the Lower Paleozoic strata, and as a result distances between the base of the intrusion and underlying Alum Shale vary significantly in the different outlier plateaus. The distance is only a few meters at the Halleberg-Hunneberg outlier, 100 meters at the Billingen-Falbygden outlier, and 180 meters at the Kinnekulle outlier (ANDERSSON *et al.*, 1985). Sampling in Västergötland was limited to the Kinnekulle outlier, which unlike the other outliers, shows no thermal effects from the overlying intrusion. A southward increase in thermal maturity on Öland also limited sampling to the thermally immature samples in the northern-most outcrops. This change in thermal maturity is attributed to increasing burial depths to the south and is not related to igneous intrusions.

The regions, localities, and biostratigraphic zones from which thermally immature samples were collected are given in Table 1. Guidelines proposed by LEWAN (1980) for the collection of unweathered samples were followed in the sampling of quarry and outcrop exposures. Although pedogenic weathering was minimal, development of fissility as a result of surface weathering was intense on some exposures. Usually, 25 to 75 cm of fissile and platy shale had to be removed from exposure faces before unweathered blocky non-fissile shale was obtained. As noted by LEWAN (1980), pyrite is extremely sensitive to outcrop weathering and its presence in a rock ensures the collection of an unweathered sample. Petrographic examination of the samples in thin sections with reflected light showed well developed euhedral pyrite with no iron-oxide rinds or pseudomorphs.

*Whole rock analyses:* The inorganic chemical components of the rocks were determined by X-ray Assay Laboratories, Inc. (Don Mills, Ontario). Except for acid-evolved $CO_2$, the major and minor oxides were determined by X-ray fluorescence spectrometry with fused lithium-tetraborate glass pellets. Total iron is expressed as FeO with a $\tau$ (tau) subscript. $CO_2$ evolved from the samples using 2N $HClO_4$ is titrated and determined with a coulometer. Total sulfur and trace elements are determined by X-ray fluorescence spectrometry with pressed powder pellets. Organic carbon was determined on a Leco carbon determinator (IR-212) after the samples were treated with 6N HCl. Thin sections of the rocks were made as outlined by LEWAN (1987).

*Kerogen analyses:* Kerogens were isolated from the rocks by a series of acid treatments involving HCl and HF, followed by a heavy-liquid separation with a zinc-bromide solution. Specifics on the procedure are given by LEWAN (1986). Elemental analyses of the isolated kerogen included determination of carbon, hydrogen, nitrogen, and oxygen. The analyses were conducted on a Carlo Erba elemental analyzer (No. 1106) with acetanilide as a standard for C, H, and N, and benzoic acid as a standard for oxygen. Visual analysis involved microscopic descriptions of kerogens dispersed in clear plastic casting resin on a glass microscope slide. Transmitted and reflected light were used to describe the kerogens at magnifications ranging from 600 to 800×. The amount of each kerogen type was determined by measuring the macerals dissected by an incremented crosshair while making traverses through the slide. Stable carbon isotopes of the kerogens were determined on HCl-decalcified and solvent-extracted rocks as described by BUCHARDT *et al.* (1986). Results are reported as per mil (‰) deviations from the PDB standard ($\delta^{13}C$) and have a reproducibility better than 0.05‰.

*Bitumen analyses:* Bitumen was obtained by extracting rock powders with dichloromethane in a Soxhlet apparatus for at least 24 hours. Whole bitumens with minor amounts of $CS_2$ were injected into a Hewlett-Packard 5996A instrument with no prior chromatographic separations. Instrument conditions and operation are discussed elsewhere by LEWAN *et al.* (1986).

*Hydrous pyrolysis experiments:* Sufficient amounts of six samples were collected for two series of hydrous pyrolysis experiments. One series of experiments involved heating each of the samples at 340°C for 72 hours. The second series of experiments involved heating aliquots of sample AS-33 for 72 hours at ten other temperatures ranging from 280 to 365°C. One-liter, stainless steel (316) reactors were filled with 400 grams of crushed rock sample ranging in size from 0.5 to 2.0 cm along with 320 grams of deionized (ASTM type I) water. The only exception to this was the experiment on sample F-2255, which was limited to 98.5 grams of crushed rock and 80 grams of deionized water in a 250 ml stainless steel (316) reactor. Headspace in all of the reactors was purged three times with 7 MPa of helium and then filled with 240 kPa of helium. Oil pyrolyzates generated and expelled from the heated rock occur in the reactor as a liquid oil layer floating on the water and to a lesser extent as a liquid oil film sorbed on the rock surfaces. The procedure for collecting this expelled oil is given elsewhere by LEWAN (1983, 1985). Gas chromatograms were obtained on the expelled oils with a Hewlett-Packard 5890 gas chromatograph. Samples were injected in the split mode at 360°C with hydrogen as the carrier gas. The oven was programmed for an initial temperature of 20°C for 5 minutes, followed by heating at 6°C/min to a final temperature of 350°C for 20 minutes. The column was a 50 m, bonded phase, fused silica, 007 methyl silicone Quadrex, with an ID of 0.25 mm and a film thickness of 0.5 $\mu$m.

*Correlation analysis:* Correlation analysis was used to examine covariations of uranium with the other measured parameters. The strength of linear bivarient covariations were quantified with the product-moment correlation coefficient ($r$) as described by HARRELL (1987). Significance of covariations was determined by the correlation coefficient for spurious correlations ($r_s$) at the 95% level (*i.e.*, $\alpha = 0.05$) based on the F test (CROW *et al.*, 1960). A verbal scale derived by HARRELL (1987) is used to describe the strength of significant correlations ($r > r_s$). The scale divides the interval between $r_s$ and a perfect correlation of 1 into five categories, with correlations coefficients being defined as *very strong* when $0.2\ r_s + 0.8 \leqq r < 1$, *strong* when $0.4\ r_s + 0.6 \leqq r < 0.2\ r_s + 0.8$, *moderate* when $0.6\ r_s + 0.4 \leqq r < 0.4\ r_s + 0.6$, *weak* when $0.8\ r_s + 0.2 \leqq r < 0.6\ r_s + 0.4$, and *very weak* when $r_s \leqq r < 0.8\ r_s + 0.2$. All significant correlations were examined by scatter plots to evaluate the influence of data points extraneous to data swarms and strong bimodal clustering of data points (HARRELL, 1984).

Table 1. Description of Thermally Immature Alum Shale Samples

| Sample | Region | Locality | Biostratigraphy |
|---|---|---|---|
| AS-8 | Kinnekulle | Trolmen Quarry | *Peltura minor* zone |
| AS-31 | Kinnekulle | Gössäter Quarry | *Peltura minor* zone |
| AS-32 | Kinnekulle | Gössäter Quarry | *Peltura minor* zone |
| AS-33 | Kinnekulle | Brattefors Quarry | *Peltura scarabaeoides* zone |
| AS-34 | Närke | Lanna Quarry | *Peltura scarabaeoides* zone |
| AS-40 | Öland | Alekinta Sea Cliff | Undifferentiated Tremadoc |
| BB-8681 | Oland | Djupvik Outcrop | *Olenus and Agnostus obesus pisiformis* zones |
| BB-8701 | Östergötland | Baarstad Core | *Dictyonema flabelliforme* zone |
| BB-8702 | Östergötland | Baarstad Core | *Leptoblastus* zone |
| BB-8703 | Östergötland | Baarstad Core | *Olenus and Agnostus obesus* zone |
| BB-8705 | Närke | Hynneberg Core | *Peltura scarabaeoides* zone |
| BB-8706 | Närke | Hynneberg Core | *Peltura minor* zone |
| BB-8707 | Närke | Hynneberg Core | *Olenus and Agnostus obesus* zone |
| F-2255 | Offshore Baltic | OPAB Well B-7 Core | Undifferentiated Upper Cambrian |

## RESULTS

*Whole rock:* X-ray diffraction powder patterns indicate that the major-mineral constituents of the samples include quartz, illite, pyrite, K-feldspar, chlorite, and a mixed layer illite-smectite. Based on this data and petrographic observations in thin sections, the rocks are classified as argillaceous claystones according to LEWAN (1978). Thin sections also indicated that the samples were thermally immature with no exogenous oil on the basis of criteria presented by LEWAN (1987). Chemical components of the rocks are given in Tables 2 and 3. Correlation analysis of these components with respect to uranium shows a weak positive correlation with Sr ($r = 0.677$), a very weak negative correlation with $SiO_2$ ($r = -0.607$), and very weak positive correlations with sulfur

**Table 2. Whole Rock Analysis of Major and Minor Oxides in Thermally Immature Samples of the Alum Shale. Concentrations are Expressed as wt %.**

| Sample Number | $SiO_2$ | $Al_2O_3$ | CaO | MgO | $Na_2O$ | $K_2O$ | $FeO^*_T$ | MnO | $TiO_2$ | $P_2O_5$ | $CO_2^+$ | S | Org.C | L.O.I.† | Total |
|---|---|---|---|---|---|---|---|---|---|---|---|---|---|---|---|
| AS-8 | 41.9 | 11.6 | 0.32 | 0.87 | 0.04 | 4.74 | 7.36 | 0.02 | 0.69 | 0.22 | <0.01 | 6.62 | 18.3 | 6.68 | 99.4 |
| AS-31 | 37.0 | 11.3 | 0.58 | 0.65 | 0.12 | 4.41 | 7.41 | 0.02 | 0.66 | 0.18 | 0.02 | 6.84 | 23.1 | 7.14 | 99.4 |
| AS-32 | 41.1 | 12.1 | 0.61 | 0.76 | 0.13 | 4.76 | 7.27 | 0.02 | 0.72 | 0.22 | <0.01 | 6.88 | 18.0 | 6.62 | 99.2 |
| AS-33 | 48.3 | 11.3 | 2.04 | 1.00 | 0.13 | 5.15 | 6.40 | 0.03 | 0.64 | 0.22 | 0.80 | 5.44 | 13.2 | 4.96 | 99.6 |
| AS-34 | 52.8 | 11.0 | 0.11 | 0.85 | 0.19 | 4.55 | 7.45 | 0.02 | 0.73 | 0.14 | <0.01 | 5.82 | 11.9 | 4.08 | 99.6 |
| AS-40 | 54.7 | 14.0 | 0.39 | 1.52 | 0.27 | 5.97 | 4.36 | 0.03 | 0.82 | 0.24 | <0.01 | 1.50 | 9.6 | 5.50 | 98.9 |
| BB-8681 | 56.7 | 9.7 | 0.14 | 1.09 | <0.01 | 3.96 | 8.57 | 0.03 | 0.58 | 0.08 | <0.01 | 5.79 | 8.6 | 4.21 | 99.5 |
| BB-8701 | 50.8 | 15.4 | 0.30 | 1.48 | <0.01 | 5.38 | 4.64 | 0.03 | 0.83 | 0.13 | IS | 2.16 | 12.4 | 6.24 | 99.8 |
| BB-8702 | 39.2 | 10.7 | 3.25 | 0.96 | <0.01 | 4.25 | 10.80 | 0.03 | 0.66 | 2.11 | IS | 9.09 | 15.7 | 2.61 | 99.4 |
| BB-8703 | 40.8 | 13.3 | 0.83 | 1.12 | <0.01 | 4.08 | 8.68 | 0.04 | 0.79 | 0.32 | 0.21 | 6.34 | 17.5 | 5.45 | 99.5 |
| BB-8705 | 45.3 | 10.9 | 0.40 | 0.97 | <0.01 | 4.34 | 7.32 | 0.03 | 0.68 | 0.15 | IS | 6.24 | 19.1 | 4.06 | 99.5 |
| BB-8706 | 42.8 | 11.7 | 0.55 | 1.10 | <0.01 | 4.37 | 7.78 | 0.03 | 0.72 | 0.27 | IS | 6.85 | 19.2 | 4.15 | 99.5 |
| BB-8707 | 45.8 | 12.2 | 0.37 | 0.83 | <0.01 | 3.92 | 6.28 | 0.03 | 0.74 | 0.10 | IS | 4.94 | 18.3 | 5.86 | 99.4 |
| F-2255 | 51.8 | 16.2 | 0.24 | 1.76 | 0.32 | 4.90 | 4.72 | 0.03 | 0.88 | 0.12 | 0.02 | 1.54 | 10.3 | 5.83 | 98.7 |

* Total iron calculated as ferrous oxide.
+ $CO_2$ evolved from sample after treatment with 2N $HClO_4$
† Weight lost on ignition at 950°C minus $CO_2$, S, and Org. C when available.
IS = insufficient sample.

($r = 0.591$) and organic carbon ($r = 0.580$). This very weak positive correlation between uranium and organic matter of the Alum Shale on a regional scale ($r = 0.580$) has also been shown on a local scale in a single core ($r = 0.39$; ARMANDS, 1972).

The proportionality of $K_2O$, $Al_2O_3$, and $SiO_2$ of the Alum Shale samples is shown in Fig. 1a on a ternary diagram with other shales of Paleozoic and Proterozoic ages. Comparisons with these shales indicate the Alum Shale samples are enriched in $K_2O$ with $Al_2O_3/K_2O$ ratios typically less than 3. This $K_2O$ enrichment is more apparent in the $Al_2O_3$-$K_2O$-[CaO + MgO + $Na_2O$] ternary diagram (Fig. 1b) with Alum Shale samples typically having $K_2O$ values greater than 20%. The Alum Shale samples are also typically enriched in $FeO_T$ (*i.e.*, total iron expressed as FeO) relative to the other shales. This is shown in the $Al_2O_3$-$FeO_T$-[CaO + MgO + $Na_2O$] ternary diagram (Fig. 1c), with all but three of the Alum Shale samples having $FeO_T$ values greater than 30%. Although the Alum Shale is typically enriched in $K_2O$ and $FeO_T$ relative to other pre-Mesozoic shales, there are no significant correlations on an absolute ($r = -0.231$) or proportional (Fig. 1) basis between these enrichments and uranium content.

*Kerogen:* Two distinct maceral types referred to as amorphous and vitrinous kerogen are identified in the visual analysis. Amorphous macerals have an irregular or diffuse outline with a mottled internal texture. Translucency and color of these macerals varies from highly translucent yellowish orange to moderately translucent orangish red. This variation in appearance is commonly observed in macerals of the same sample or within the same maceral, and are the result of variations in maceral thickness and not radiation damage. Polished sections under reflected light show this maceral to have a speckled nonuniform reflectance. As shown in Table 4, this maceral type accounts for 80 to 98 volume percent of the kerogen and ranges in mean size from 11 to 56 μm. The predominance of this maceral type gives its abundance in terms of weight percent of rock (Table 4), a very weak correlation with uranium ($r = 0.581$) that is similar to the correlation between organic carbon and uranium ($r = 0.580$).

Vitrinous macerals have sharp outlines, angular shapes, and smooth structureless internal textures. Similar to amorphous macerals, their translucency and color varies from highly translucent yellowish orange to moderately translucent orangish red with increasing thickness. Polished sections under reflected light show this maceral to have a uniform gray reflectance similar to vitrinite (BUCHARDT and LEWAN, 1989). As shown in Table 4, vitrinous macerals account for 2 to 20 volume percent of the kerogen and range in mean size from 3 to 6 μm. Variations in the amount of this maceral on a whole rock basis show no significant correlation with uranium ($r = 0.417$). Mean reflectance values of these vitrinite-like macerals range from 0.32 to 0.52% $R_0$ (Table 5) and are indicative of thermal immaturity (BUCHARDT and LEWAN, 1989). This subtle variation in reflectance values shows no significant correlation with uranium content ($r = 0.454$).

$\delta^{13}C$ values of the kerogens range from −27.5 to −30.1‰ (Table 5). These values are within the range previously reported for the Alum Shale (BUCHARDT *et al.*, 1986) and are depleted in $^{13}C$ relative to organic matter in modern open-marine systems (LEWAN, 1986). The variations in the isotopic values have no significant correlation with the volume percent of maceral types in the kerogen ($r = \pm 0.168$), but do have a very weak positive correlation with the organic carbon content of the rocks ($r = 0.625$). There is no significant correlation between $\delta^{13}C$ of the kerogens and uranium ($r = 0.376$).

**Table 3. Whole Rock Analyses of Trace Elements in Thermally Immature Samples of Alum Shale. Concentrations are Expressed as ppm.**

| Sample Number | U | Th | Rb | Sr | Ba | Cr | Y | Zr | Nb | Cl | Se |
|---|---|---|---|---|---|---|---|---|---|---|---|
| AS-8 | 180 | 10 | 240 | 80 | 1090 | 130 | 30 | 120 | 20 | 100 | 12 |
| AS-31 | 190 | 12 | 200 | 70 | 760 | 170 | 30 | 100 | 10 | 200 | 12 |
| AS-32 | 440 | 8 | 240 | 120 | 810 | 160 | 30 | 130 | <10 | 200 | 30 |
| AS-33 | 150 | 10 | 200 | 120 | 580 | 170 | 60 | 110 | 10 | <50 | 9 |
| AS-34 | 190 | 12 | 200 | 50 | 510 | 180 | 30 | 170 | 10 | 50 | 9 |
| AS-40 | 60 | 12 | 240 | 50 | 680 | 210 | 20 | 150 | 10 | <50 | 21 |
| BB-8681 | 18 | <2 | 160 | 20 | 420 | 270 | <10 | 120 | 20 | 350 | 9 |
| BB-8701 | 130 | 20 | 230 | 110 | 540 | 200 | 60 | 140 | 20 | 100 | 6 |
| BB-8702 | 370 | 4 | 200 | 160 | 440 | 200 | 140 | 110 | 10 | 50 | 9 |
| BB-8703 | 120 | 12 | 220 | 70 | 520 | 140 | 30 | 150 | 20 | 150 | 6 |
| BB-8705 | 420 | 12 | 200 | 90 | 470 | 410 | 40 | 130 | <10 | 150 | 9 |
| BB-8706 | 260 | 14 | 210 | 120 | 510 | 270 | 60 | 140 | <10 | 50 | 18 |
| BB-8707 | 180 | 10 | 230 | 80 | 520 | 200 | 20 | 120 | 10 | 250 | 18 |
| F-2255 | 110 | 18 | 180 | 60 | 510 | 140 | 30 | 150 | 20 | <50 | 12 |

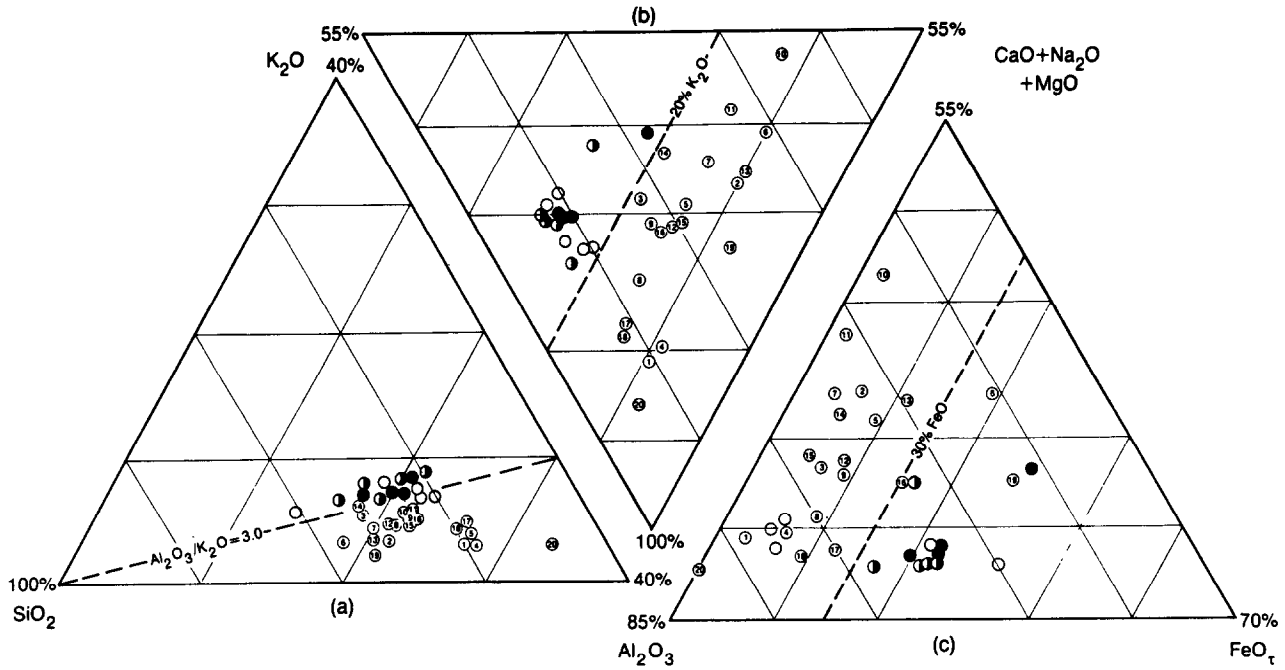


FIG. 1. Ternary chemical-component diagrams of (a) $K_2O$-$SiO_2$-$Al_2O_3$, (b) $K_2O$-$Al_2O_3$-[CaO + $Na_2O$ + MgO], and (c) [CaO + $Na_2O$ + MgO]-$Al_2O_3$-$FeO_T$ of the Alum Shale (○, U < 150 ppm; ◑, U = 150–250 ppm; ●, U = 250–450 ppm) and other fine-grained sedimentary rocks (*1*, mean of 17 samples of Hepworth Carboniferous shales and mudstones, PEARSON, 1979; *2*, mean of 8 samples of Archean shales from the Canadian Shield, CAMERON and GARRELS, 1980; *3*, mean of 6 samples of Aphebian shales from the Canadian Shield, CAMERON and GARRELS, 1980; *4*, mean of 25 samples of nonmarine Namurian black shales, SPEARS and AMIN, 1981; *5*, mean of 19 marine Namurian black shales, SPEARS and AMIN, 1981; *6*, mean of 5 samples of Fig Tree shales, MCLENNAN and TAYLOR, 1983; *7*, North American shale composite, GROMET *et al.*, 1984; *8*, mean of 7 samples of Devonian Littleton shales, SHAW, 1956; *9*, mean of 34 samples of Late Proterozoic clays and shales from the Russian platform, RONOV and MIGDISOV, 1971; *10*, mean of 401 samples of Paleozoic clays and shales from the Russian platform, RONOV and MIGDISOV, 1971; *11*, mean of 473 analyses of Paleozoic clays and shales from the North American platform, RONOV and MIGDISOV, 1971; *12*, composite sample of 51 Paleozoic shales, CLARKE, 1924; *13*, mean of 19 samples of the Nonesuch Parting Shale, WIESE, 1973; *14*, weighted mean of 348 samples of shales from the New Albany Shale Group, FROST *et al.*, 1985; *15*, mean of 36 samples of American roofing slates, ECKEL, 1904; *16*, mean of 33 samples of Precambrian lutites, NANZ, 1953; *17*, mean of 15 marine shales of Pennsylvanian age, KEITH and DEGENS, 1959; *18*, mean of 15 fresh-water shales of Pennsylvanian age, KEITH and DEGENS, 1959; *19*, mean of 22 samples of Witwatersrand Supergroup shales, WRONKIEWICZ and CONDIE, 1987; *20*, mean of 9 samples of Carboniferous shales and mudstones from South Yorkshire, SPEARS and SEZGIN, 1985).

Standardized weight percentages of the carbon, hydrogen, nitrogen, and oxygen content of the kerogens are given in Table 5. The atomic H/C and O/C ratios indicate these are type II kerogens in accordance with the classification by TISSOT *et al.* (1974). The atomic H/C ratios have a considerable range of values for thermally immature kerogens. This vari-

**Table 4. Visual Analysis of Kerogens from Samples of Thermally Immature Alum Shale**

| Sample Number | Kerogen Types (vol.% of Kerogen) Amorphous | Vitrinous | Mean Maceral Size (μm) Amorphous | Vitrinous | Total Number of Macerals Measured | Kerogen Types† (wt.% of Rock) Amorphous | Vitrinous |
|---|---|---|---|---|---|---|---|
| AS-8 | 90.7 | 9.3 | 12 | 3 | 101 | 22.6 | 2.1 |
| AS-31 | 79.8 | 20.2 | 15 | 4 | 100 | 27.5 | 5.5 |
| AS-32 | 89.3 | 10.7 | 11 | 3 | 114 | 22.2 | 2.4 |
| AS-33 | 95.4 | 4.6 | 18 | 5 | 93 | 16.0 | 0.8 |
| AS-34 | 94.8 | 5.2 | 18 | 4 | 116 | 14.5 | 0.8 |
| AS-40 | 93.9 | 6.1 | 16 | 3 | 115 | 11.9 | 0.7 |
| BB-8681 | 84.8 | 15.2 | 22 | 5 | 134 | 10.5 | 1.6 |
| BB-8701 | 91.7 | 8.3 | 27 | 5 | 103 | 14.8 | 1.2 |
| BB-8702 | 90.8 | 9.2 | 17 | 4 | 100 | 18.7 | 1.7 |
| BB-8703 | 92.4 | 7.6 | 21 | 4 | 94 | 21.0 | 0.6 |
| BB-8705 | 85.3 | 14.7 | 15 | 5 | 108 | 22.6 | 3.3 |
| BB-8706 | 92.6 | 7.4 | 24 | 5 | 76 | 22.7 | 1.7 |
| BB-8707 | 95.7 | 4.3 | 29 | 4 | 79 | 21.8 | 0.9 |
| F-2255 | 97.8 | 2.2 | 56 | 6 | 85 | 12.2 | 0.3 |

† Weight percent of kerogen type in rock = $\frac{\text{Wt.\% Org.C in Rock}}{\text{Wt.\% C in Kerogen}}$ x vol. % in kerogen. This assumes the bulk densities of both macerals are the same.

Table 5. Reflectance, Carbon Isotope, and Elemental Data of Kerogens from Samples of Thermally Immature Alum Shale

| Sample Number | Reflectance (%$R_o$) Mean | Std. Dev | Counts | $\delta^{13}C$ (o/oo, PDB) | Elemental Analysis (wt. %) C | H | N | O | Atomic Ratios H/C | O/C |
|---|---|---|---|---|---|---|---|---|---|---|
| AS-8 | 0.50 | 0.08 | 52 | -29.1 | 83.9 | 7.5 | 1.4 | 7.2 | 1.07 | 0.06 |
| AS-31 | 0.49 | 0.04 | 52 | -28.7 | 83.9 | 8.0 | 1.5 | 6.6 | 1.14 | 0.06 |
| AS-32 | 0.52 | 0.04 | 70 | -28.2 | 81.2 | 7.1 | 1.3 | 10.4 | 1.05 | 0.10 |
| AS-33 | 0.52 | 0.05 | 70 | -29.2 | 82.7 | 7.5 | 1.8 | 8.0 | 1.09 | 0.07 |
| AS-34 | 0.49 | 0.04 | 45 | -28.8 | 82.1 | 7.9 | 1.6 | 8.4 | 1.15 | 0.08 |
| AS-40 | 0.47 | 0.05 | 75 | -29.9 | 80.4 | 7.8 | 2.5 | 9.3 | 1.16 | 0.09 |
| BB-8681 | 0.32 | 0.05 | 70 | -30.1 | 81.8 | 7.9 | 2.8 | 7.5 | 1.16 | 0.07 |
| BB-8701 | 0.48 | 0.06 | 70 | -28.8 | 83.7 | 7.9 | 2.0 | 6.4 | 1.13 | 0.06 |
| BB-8702 | 0.51 | 0.05 | 70 | -29.9 | 84.0 | 7.1 | 1.4 | 7.5 | 1.01 | 0.07 |
| BB-8703 | 0.53 | 0.09 | 70 | -27.5 | 83.4 | 7.8 | 1.9 | 6.9 | 1.12 | 0.06 |
| BB-8705 | 0.51 | 0.13 | 70 | -28.5 | 84.6 | 7.1 | 1.5 | 6.8 | 1.01 | 0.06 |
| BB-8706 | 0.44 | 0.10 | 70 | -28.4 | 84.7 | 7.6 | 1.6 | 6.1 | 1.08 | 0.05 |
| BB-8707 | 0.44 | 0.09 | 70 | -29.3 | 83.9 | 7.8 | 1.7 | 6.6 | 1.12 | 0.06 |
| F-2255 | 0.51 | 0.10 | 75 | -30.0 | 84.6 | 8.0 | 2.5 | 4.9 | 1.13 | 0.04 |

ation does not have a significant correlation with the variations in the two maceral types ($r = \pm 0.134$) or the reflectance values of the vitrinite-like macerals ($r = -0.441$). However, it does have a strong negative correlation ($r = -0.871$) with uranium. As shown in Fig. 2a, atomic H/C ratios of the kerogens decrease as the uranium contents of the rocks increase. Within the range of these values (*i.e.*, 1.00 to 1.20), the analytical error for atomic H/C ratios is ±0.03.

*Bitumen extract:* The amount of bitumen extract and its proportionality to organic carbon range from 510 to 3845 ppm and 0.0028 to 0.0447, respectively (Table 6). Positive correlations between the atomic H/C ratio of the kerogens and variations in bitumen content and bitumen/organic carbon ratio are significant but weak ($r = 0.646$) and very weak ($r = 0.613$), respectively. This is peculiar from the standpoint of thermal maturity, which usually shows an initial increase

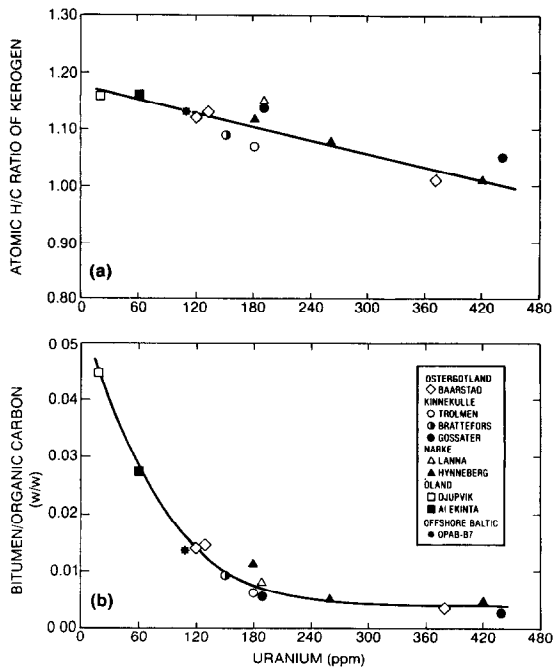


FIG. 2. (a) Plot showing linear relationship between atomic H/C ratio of kerogens and uranium content of rocks. The regression line is described by the equation $H/C = -39.43 \cdot 10^{-5} U + 1.177$, which has a correlation coefficient of −0.871. (b) Plot showing curvilinear relationship between bitumen/organic carbon ratio and uranium content of thermally immature Alum Shale samples.

Table 6. Amount of Bitumen Extract and Distribution of Its Acyclic Alkanes. Alkane Ratios are Based on Peak Heights from m/z 57 Ion Chromatograms of Whole Bitumen

| Sample Number | Bitumen (ppm) | Bitumen / Org. Carbon | CPI† (20–28) | Pristane+Phytane / $n\text{-}C_{17}+n\text{-}C_{18}$ | Pristane / Phytane | Bitumen Type |
|---|---|---|---|---|---|---|
| AS-8 | 1086 | 0.0059 | n.d. | n.d | n.d. | n.d. |
| AS-31 | 1267 | 0.0055 | 0.92 | 0.22 | 1.20 | A |
| AS-32 | 510 | 0.0028 | 0.88 | 0.36 | 0.97 | B |
| AS-33 | 1192 | 0.0090 | 0.91 | 0.27 | 1.17 | A |
| AS-34 | 965 | 0.0081 | n.d. | n.d. | n.d | n.d |
| AS-40 | 2620 | 0.0273 | 0.99 | 0.28 | 1.44 | A |
| BB-8681 | 3845 | 0.0447 | 0.97 | 0.95 | 1.98 | A |
| BB-8701 | 1818 | 0.0147 | 0.95 | 0.42 | 0.83 | B |
| BB-8702 | 880 | 0.0056 | 0.94 | 0.42 | 0.90 | B |
| BB-8703 | 2425 | 0.0139 | 0.94 | 0.39 | 1.28 | A |
| BB-8705 | 955 | 0.0050 | 0.93 | 0.46 | 0.75 | B |
| BB-8706 | 1005 | 0.0052 | 0.94 | 0.37 | 0.86 | B |
| BB-8707 | 2038 | 0.0111 | 0.97 | 0.39 | 0.89 | B |
| F-2255 | 1367 | 0.0133 | 1.05 | 0.19 | 1.56 | A |

$$\text{†CPI} = 0.5\left[\frac{C_{21}+C_{23}+C_{25}+C_{27}}{C_{20}+C_{22}+C_{24}+C_{26}} + \frac{C_{21}+C_{23}+C_{25}+C_{27}}{C_{22}+C_{24}+C_{26}+C_{28}}\right]$$

n.d. = not determined

in bitumen with a corresponding decrease in the kerogen H/C ratio (TISSOT and WELTE, 1978, pp. 467 and 468; LEWAN, 1983; HARWOOD, 1977). Another peculiar aspect is the lack of a significant positive correlation between the amounts of bitumen and organic carbon ($r = -0.517$), which usually exists for samples at similar levels of thermal maturity from the same source rock (TISSOT and WELTE, 1978, p. 165). Uranium has a significant negative correlation with the amount of bitumen ($r = -0.762$) and the bitumen/organic carbon ratio ($r = -0.715$). As shown in Fig. 2b, this correlation is actually curvilinear with bitumen/organic-carbon ratios becoming asymptotic between values of 0.003 and 0.005 at uranium concentrations greater than 200 ppm.

Eleven of the bitumen extracts were analyzed by gas chromatography/mass spectrometry (GC/MS). Two distinct alkane distributions are apparent from the m/z 57 ion chromatograms (Fig. 3). Type-A bitumens have smooth exponentially decreasing *n*-alkane distributions with pristane/phytane ratios greater than one (Fig. 3, Table 6), and Type-B bitumens have bimodal normal-alkane distributions with maxima at $n\text{-}C_{18}$ and $n\text{-}C_{22}$ (Fig. 3) and pristane/phytane ratios less than one (Table 6). Type-A bitumens are more

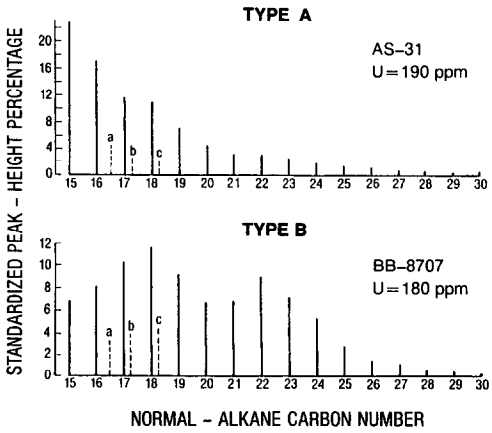


FIG. 3. *N*-alkane and acyclic isoprenoid distributions of Type-A and Type-B bitumens. The standardized peak-height percentages were determined from m/z 57 ion chromatograms. The broken lines labeled a, b, and c are norpristane, pristane, and phytane, respectively.

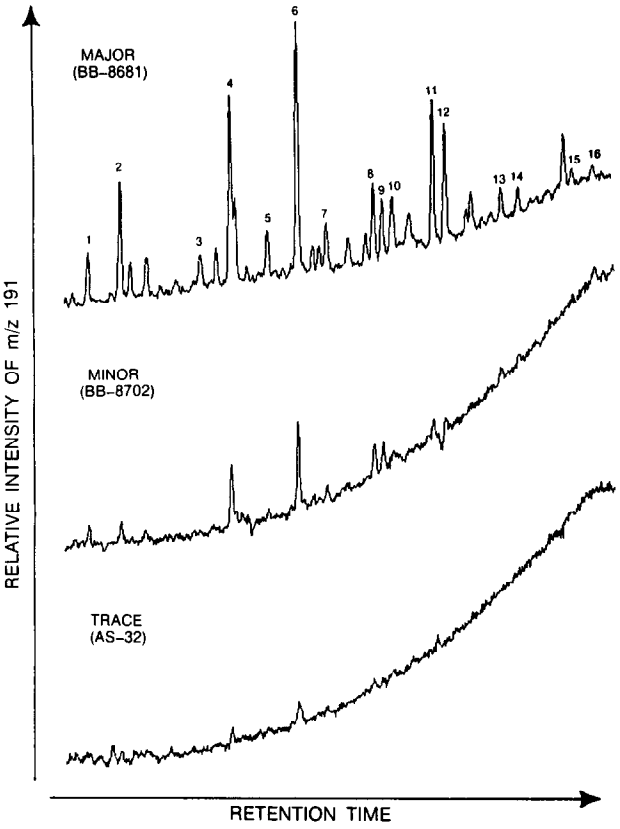


FIG. 4. The m/z 191 ion chromatograms representing the different concentrations of pentacyclic terpanes relative to background. Labeled peaks have been identified as *1* = 18$\alpha$-trisnorneohopane (Ts); *2* = 17$\alpha$-trisnorhopane (Tm); *3* = 17$\alpha$,18$\beta$,21$\beta$-28,30-bisnorhopane; *4* = 17$\alpha$,21$\beta$-norhopane; *5* = 17$\beta$,21$\alpha$-norhopane; *6* = 17$\alpha$,21$\beta$-hopane; *7* = 17$\beta$,21$\alpha$-hopane; *8* = 17$\alpha$,21$\beta$-homohopane (22S); *9* = 17$\alpha$,21$\beta$-homohopane (22R); *10* = gammacerane; *11* = 17$\alpha$,21$\beta$-bishomohopane (22S); *12* = 17$\alpha$,21$\beta$-bishomohopane (22R); *13* = 17$\alpha$,21$\beta$-trishomohopane (22S); *14* = 17$\alpha$,21$\beta$-trishomohopane (22R); *15* = 17$\alpha$,21$\beta$-tetrakishomohopane (22S); and *16* = 17$\alpha$,21$\beta$-tetrakishomohopane (22R).

commonly associated with rocks having low uranium concentrations (<200 ppm), but there is sufficient overlap in the range of uranium concentrations between the two bitumen types (120 to 200 ppm) to question the significance of a relationship. Collectively, the pristane/phytane ratios of both bitumen types have a moderate positive correlation with the bitumen/organic carbon ratios ($r$ = 0.818). This type of relationship is usually attributed to thermal maturation with bitumen/organic carbon and pristane/phytane ratios increasing as the thermal stress experienced by a rock increases (TISSOT *et al.*, 1971). The proportionality of pristane and phytane to $n$-$C_{17}$ and $n$-$C_{18}$ alkanes is less variable for Type-B bitumens (0.36 to 0.46, Table 6) than for Type-A bitumens (0.19 to 0.95, Table 6). This parameter usually decreases with increasing thermal stress (LIJMBACH, 1975). Although there is a moderate negative correlation between this parameter and variations in the $\%R_0$ reflectance values ($r$ = −0.788), the parameter does not have a significant correlation with variations in the pristane/phytane ratios ($r$ = −0.391).

Carbon preference indices (CPI) for both bitumen types have an even-carbon predominance except for sample F-2255 (Table 6). This index is expected to approach unity with increasing thermal stress, but it does not have a significant correlation with the $\%R_0$ reflectance values ($r$ = −0.257). $N$-alkane distributions with an even predominance are attributed to highly reducing diagenetic environments, which also result in pristane/phytane ratios less than one (TISSOT and WELTE, 1978, pp. 105–107). Contrary to this generalization, the CPI values have a weak negative correlation with the total sulfur content of the rock ($r$ = −0.681) and no significant correlation with the pristane/phytane ratios ($r$ = 0.498). CPI values have a very-weak negative correlation with uranium content ($r$ = −0.590).

The concentrations of hopanes relative to background in the m/z 191 ion chromatogram vary considerably among the bitumen extracts. A qualitative assessment of these relative concentrations is given in Fig. 4. Table 7 shows that major concentrations of hopanes only occur in the two samples with the lowest uranium contents (BB-8681 and AS-40). Hopane distributions of these two samples are similar with the only major difference being the abundant bishomohopanes in sample BB-8681. The distribution of $C_{31}$- through $C_{33}$-hopanes in sample AS-40 has the typical smooth exponential decrease with increasing carbon number. Gammacerane occurs in both samples and is considered to be indicative of hypersaline environments (TEN HAVEN *et al.*, 1985; JIAMO *et al.*, 1985). The low concentrations of hopanes in most of

**Table 7. Data on the Hopanes from the m/z 191 Ion Chromatogram, Steranes from the m/z 217 Ion Chromatogram, and Triaromatic Steroid Hydrocarbons from the m/z 231 Ion Chromatogram Given in Order of Increasing Uranium Content**

| Sample Number | Uranium (ppm) | Hopanes Relative Abundance | Hopanes Ts/Tm | Steranes Distribution Type | Steranes 20S/(20S + 20R) | Triaromatic Steroids $(C_{20}+C_{21})/(C_{20}+C_{21}+C_{26}+C_{27}+C_{28})$ | Triaromatic Steroids $(C_{28})/(C_{26}+C_{27}+C_{28})$ |
|---|---|---|---|---|---|---|---|
| BB-8681 | 18 | M | 0.44 | I | 0.21 | 0.13 | 0.58 |
| AS-40 | 60 | M | 0.53 | I | 0.18 | 0.22 | 0.56 |
| F-2255 | 110 | t | n.d. | II | 0.20 | 0.75 | 0.42 |
| BB-8703 | 120 | m | 0.63 | II | 0.22 | 0.47 | 0.45 |
| BB-8701 | 130 | m | 0.78 | II | 0.31 | 0.64 | 0.40 |
| AS-33 | 150 | t | n.d. | II | 0.25 | 0.72 | 0.36 |
| BB-8707 | 180 | t | n.d. | I | n.d. | 0.67 | 0.39 |
| AS-31 | 190 | t | n.d. | II | 0.19 | 0.75 | 0.35 |
| BB-8706 | 260 | m | 0.73 | I | 0.14 | 0.76 | 0.33 |
| BB-8702 | 370 | m | 1.00 | I | 0.36 | 0.68 | 0.36 |
| BB-8705 | 420 | m | 1.04 | I | 0.37 | 0.67 | 0.40 |
| AS-32 | 440 | t | n.d. | n.d. | n.d. | 1.00 | n.d. |

n.d. = not determined
t = trace
M = Major
m = minor

the samples limit the study of m/z 191 ion chromatograms to the $C_{27}$ triterpane ratio (Ts/Tm). This ratio increases with increasing thermal stress and has been used as a thermal maturity index (SEIFERT and MOLDOWAN, 1978; HUGHES *et al.*, 1985). Table 7 shows this ratio to vary from 0.44 to 1.04, and to have a strong positive correlation with uranium content ($r = 0.949$). Although the strong negative correlation of this ratio with atomic H/C ratios of the kerogen ($r = -0.938$) is suggestive of increasing thermal stress, the moderate and weak negative correlations of this ratio with bitumen content ($r = -0.893$) and bitumen/organic carbon ratio ($r = -0.837$) do not support such an interpretation.

Steroid hydrocarbon distributions in the m/z 217 ion chromatogram are classified into two types as shown in Fig. 5. Type-I has a full range of $C_{27}$ through $C_{29}$ diasteranes and steranes, with 24-ethyl-14$\alpha$,17$\alpha$-cholestane (20R) having the greatest intensity. Type-II has no detectable $C_{27}$ diasteranes or steranes, with 24-methyl-14$\alpha$,17$\alpha$-cholestane (20R) having the greatest intensity. These two types of distributions show no correlation with the Type-A and -B alkane distributions. Table 7 shows there is no relationship between these two sterane distributions and uranium content. The dominance of the 20R isomer over the 20S isomer of 24-ethyl-14$\alpha$,17$\alpha$-cholestane occurs in both of the sterane distributions (Table 7). This suggests thermal immaturity, which agrees with the $\%R_0$ reflectance values. Variations in the decimal fraction of these two isomers have no significant correlation with uranium content ($r = 0.628$).

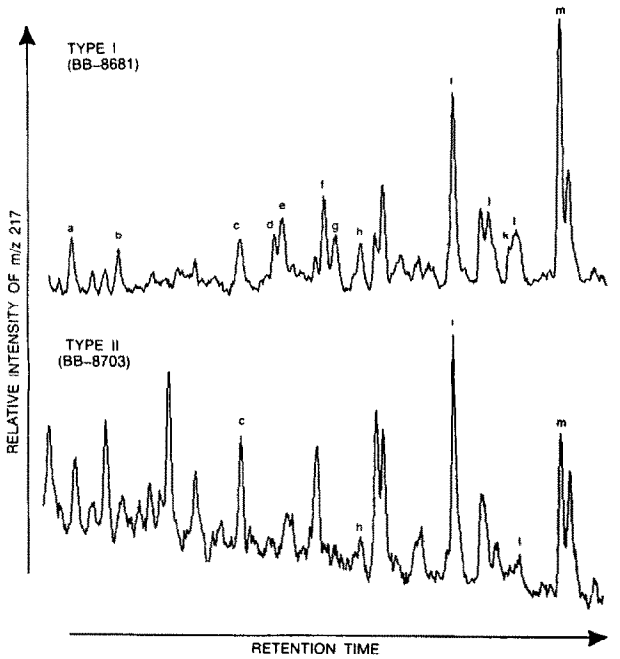


FIG. 5. The m/z 217 ion chromatograms showing the two types of sterane distributions of bitumen extracts. Labeled peaks have been identified as $a$ = 13$\beta$,17$\alpha$-diacholestane (20S); $b$ = 13$\beta$,17$\alpha$-diacholestane (20R); $c$ = 24-methyl-13$\beta$,17$\alpha$-diacholestane (20R); $d$ = 24-methyl-13$\alpha$,17$\beta$-diacholestane (20S) + 14$\alpha$,17$\alpha$-cholestane (20S); $e$ = 24-methyl-13$\beta$,17$\alpha$-diacholestane (20S) + 14$\alpha$,17$\beta$-cholestane (20R); $f$ = 14$\alpha$,17$\alpha$-cholestane (20R); $g$ = 24-ethyl-13$\beta$,17$\alpha$-diacholestane (20R); $h$ = 24-ethyl-13$\alpha$,17$\beta$-diacholestane (20S); $i$ = 24-methyl-14$\alpha$,17$\alpha$-cholestane (20R); $j$ = 24-ethyl-14$\alpha$,17$\alpha$-cholestane (20S); $k$ = 24-ethyl-14$\beta$,17$\beta$-cholestane (20R); $l$ = 24-ethyl-14$\beta$,17$\beta$-cholestane (20S); and $m$ = 24-ethyl-14$\alpha$,17$\alpha$-cholestane (20R).

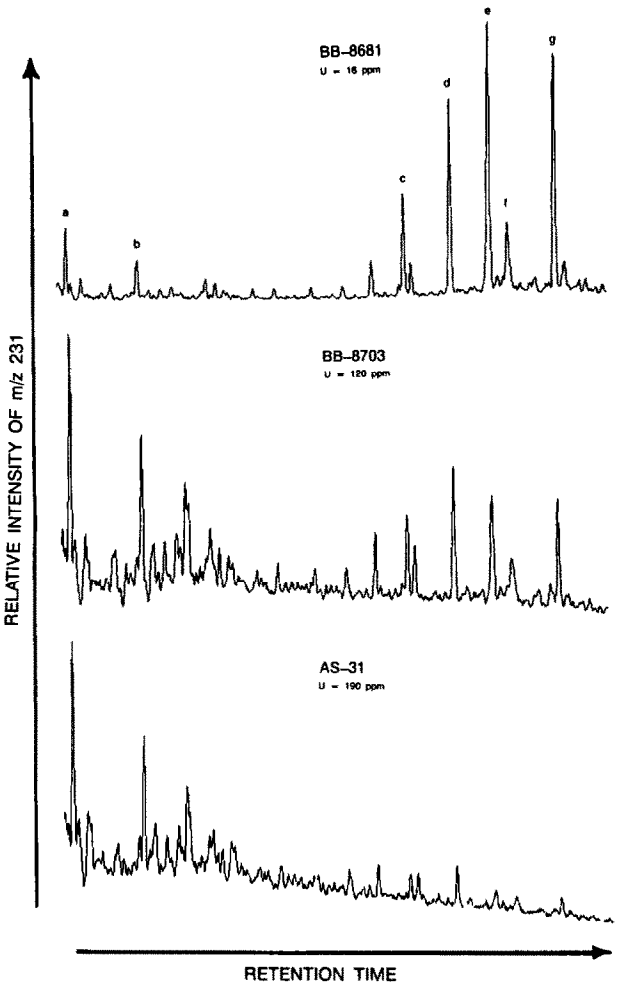


FIG. 6. The m/z 231 ion chromatograms showing changes in the distribution of triaromatic steroid hydrocarbons with uranium content of rock. Labeled peaks have been identified as $a$ = $C_{20}$-triaromatic, $b$ = $C_{21}$-triaromatic, $c$ = $C_{26}$-triaromatic (20S), $d$ = $C_{26}$-triaromatic (20R) + $C_{27}$-triaromatic (20S), $e$ = $C_{28}$-triaromatic (20S), $f$ = $C_{27}$-triaromatic (20R), and $g$ = $C_{28}$-triaromatic (20R).

The m/z 231 ion chromatograms show considerable variability between the low- and high-molecular weight triaromatic steroid hydrocarbons (Fig. 6). This is expressed as a decimal fraction (*i.e.*, $[C_{20} + C_{21}]/[C_{20} + C_{21} + C_{26} + C_{27} + C_{28}]$), which increases with increasing thermal stress from values of less than 0.10 to 1.0. Table 7 shows this parameter to vary from 0.13 to 1.00 in spite of the uniform low thermal stress experienced by the samples. This parameter has no significant correlation with atomic H/C ratio of the kerogens ($r = -0.561$). In contrast to normal thermal maturity trends, this triaromatic ratio has a strong negative correlation with the bitumen/organic carbon ratio ($r = -0.902$). Similar to the bitumen/organic carbon ratio (Fig. 2b), the triaromatic ratio has a significant correlation ($r = 0.70$) with uranium content, which is better expressed as a curvilinear relationship (Fig. 7a). Changes occur within the distribution of high-molecular weight triaromatics as the relative concentration of

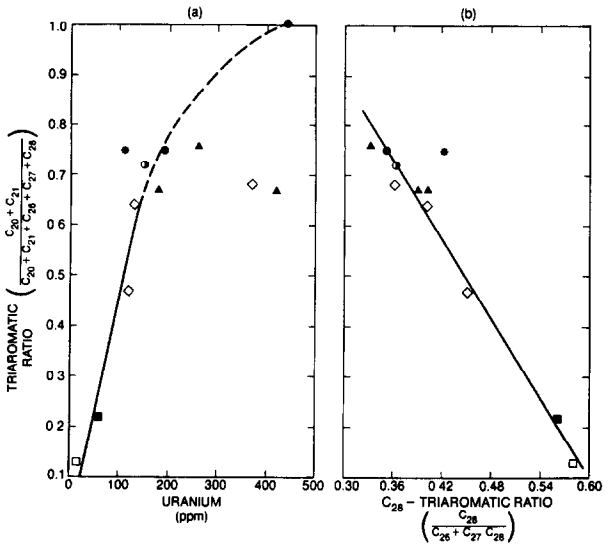


FIG. 7. Plots showing the triaromatic side-chain cleavage ratio ($[C_{20} + C_{21}]/[C_{20} + C_{21} + C_{26} + C_{27} + C_{28}]$) *versus* (a) uranium content of rock, and (b) relative abundance of $C_{28}$-triaromatics ($C_{28}/[C_{26} + C_{27} + C_{28}]$). Symbol designation is given in Fig. 2.

low-molecular weight triaromatics increase. This change is expressed in Table 7 as a decimal fraction of the $C_{28}$-triaromatic over the sum of $C_{26}$ through $C_{28}$ triaromatics (*i.e.*, $C_{28}/[C_{26} + C_{27} + C_{28}]$). Figure 7b shows the strong negative correlation ($r = -0.959$) between this parameter and the triaromatic ratio.

*Expelled-oil pyrolyzates:* The six samples of which sufficient amounts of rock were available for hydrous pyrolysis experiments gave variable expelled-oil yields at 340°C after 72 hours. Table 8 shows that under these conditions, the amount of expelled oil relative to organic carbon ranges from 6.59 to 17.62. This variability has a curvilinear relationship with uranium content as shown in Fig. 8. The series of hydrous pyrolysis experiments conducted on sample AS-33 shows an increase in expelled oil with increasing temperature and a maximum yield relative to organic carbon of 18.32 at 360°C after 72 hours (Table 8). This maximum yield is considerably less than the 24.73 and 27.63 maximum yields reported for the Woodford Shale and Phosphoria Retort Shale, respectively (LEWAN, 1985).

Table 8. Data on Amount and Character of Oils Expelled from Thermally Immature Alum Shale Samples in Hydrous Pyrolysis Experiments

| Sample Number | Experimental* Temperature (°C) | Expelled Oil (wt. % of Rock) | Expelled Oil x 100 / Organic Carbon | n-C11 Index** |
|---|---|---|---|---|
| AS-31 | 340 | 2.11 | 9.15 | 21.18 |
| AS-32 | 340 | 1.19 | 6.59 | 24.82 |
| AS-33 | 340 | 1.30 | 9.86 | 19.87 |
| AS-40 | 340 | 1.69 | 17.62 | 17.26 |
| BB-8681 | 340 | 1.25 | 14.56 | 15.30 |
| F-2255 | 340 | 1.47 | 14.31 | 18.59 |
| AS-33 | 280 | 0.03 | 0.20 | *** |
| AS-33 | 300 | 0.13 | 0.99 | 25.53 |
| AS-33 | 310 | 0.29 | 2.17 | 24.57 |
| AS-33 | 320 | 0.62 | 4.66 | 22.61 |
| AS-33 | 330 | 1.05 | 7.98 | 21.06 |
| AS-33 | 345 | 1.66 | 12.56 | 20.92 |
| AS-33 | 350 | 2.02 | 15.32 | 19.57 |
| AS-33 | 355 | 2.11 | 15.98 | 18.77 |
| AS-33 | 360 | 2.42 | 18.32 | 17.37 |
| AS-33 | 365 | 2.39 | 18.13 | 17.47 |

* All experiments are for 72 hours.

** $n\text{-}C_{11}$ index $= \dfrac{nC_{11} \times 100}{\Sigma(nC_{10} \text{ through } nC_{30})}$

*** Could not be determined due to loss of light ends.

Gas chromatograms of the expelled oils show considerable variability ranging from normal oils with *n*-alkane distributions between $C_7$ and $C_{31}$ and acyclic isoprenoids to condensate-like oils with *n*-alkane distributions between $C_5$ and $C_{12}$ and no acyclic isoprenoids (Fig. 9). The differences in alkane distributions are expressed as the percent of $n\text{-}C_{11}$ in the *n*-alkane distribution from $C_{10}$ through $C_{30}$ (*i.e.*, $[n\text{-}C_{11} \times 100]/\Sigma[n\text{-}C_{10}$ through $n\text{-}C_{30}]$). As the distribution becomes more condensate-like the $n\text{-}C_{11}$ index increases. The variability of this index for the expelled oils from the different samples at 340°C after 72 hours is shown in Table 8. Figure 10 shows there is a curvilinear relationship between the $n\text{-}C_{11}$ index and uranium content, with more condensate-like oils being generated from rocks with high uranium contents. Expelled oils from the series of hydrous pyrolysis experiments on sample AS-33 at different temperatures are less condensate-like with increasing thermal stress ($n\text{-}C_{11}$ index, Table 8). This is contrary to thermal maturation trends, which usually show the reverse.

Assuming a first-order rate law, the overall kinetics for generation of expelled oil from sample AS-33 at different temperatures were determined (*e.g.*, LEWAN, 1985). An Arrhenius plot of the data in Fig. 11 shows a linear relationship ($r = -0.997$) that is described by one set of kinetic parameters, with an activation energy ($E_A$) of 201.3 kJ mol$^{-1}$ and a pre-

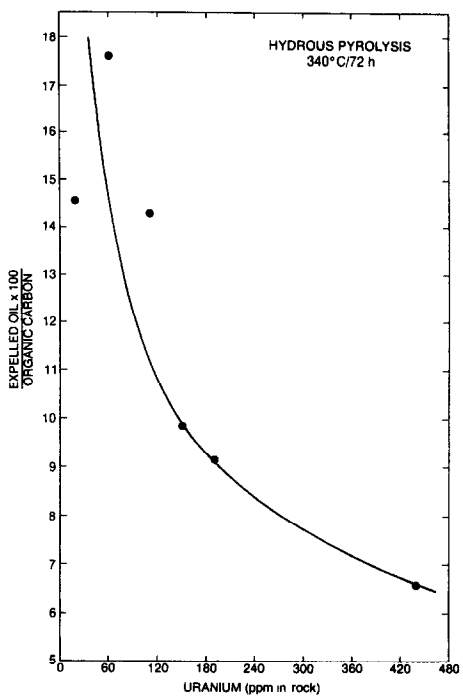


FIG. 8. Plot of expelled oil *versus* uranium content of thermally immature samples of Alum Shale (Table 8). Expelled oils are expressed relative to the organic carbon content of the samples and were generated by hydrous pyrolysis at 340°C after 72 hours.

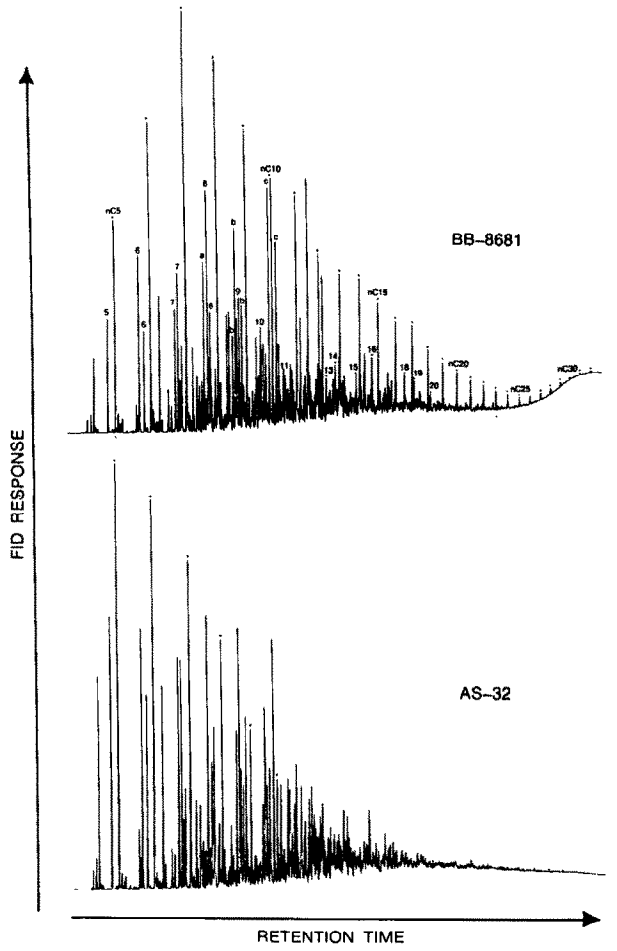


FIG. 9. Chromatograms showing the two extremes in *n*-alkane distributions of expelled oils generated by hydrous pyrolysis at 340°C after 72 hours from Alum Shale samples. Peaks representing normal alkanes are dotted with those having carbon numbers divisible by five labeled. Numbers over peaks designate the carbon number of branched acyclic alkanes. Peaks designated as *a* = toluene, *b* = $C_2$ substituted benzenes, and *c* = $C_3$ substituted benzenes.

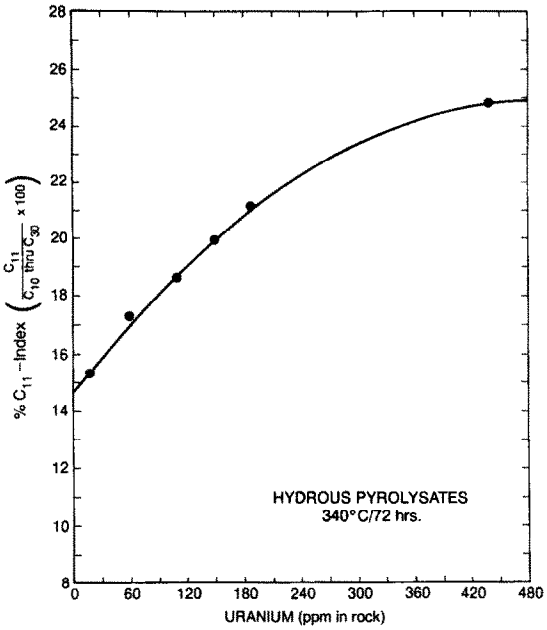


FIG. 10. Plot showing the increase in $n$-$C_{11}$ index of expelled oils with increasing uranium content of thermally immature samples. The expelled oils are products of hydrous pyrolysis experiments that were conducted at 340°C for 72 hours.

exponential factor ($A_0$) of $1.77 \cdot 10^{15}$ $hr^{-1}$. These values are intermediate to those reported by LEWAN (1985) for the Woodford Shale and Phosphoria Retort Shale as shown in Table 9. LEWAN (1985) concludes that the difference in kinetics between Woodford Shale and Phosphoria retort Shale is in part related to the amount of organic sulfur in the original kerogens. As shown in Table 9, the organic sulfur content of sample AS-33 falls intermediate to the other two shales and supports this general concept.

## DISCUSSION

*Evidence of radiation damage:* Expelled oils generated by hydrous pyrolysis provide the most convincing evidence that radiation damage to organic matter in the Alum Shale has occurred. Generation of condensate-like oils from thermally immature organic-rich rocks under hydrous-pyrolysis conditions at 340°C after 72 hours is not typical. As monitored by the $n$-$C_{11}$ index, the increase in condensate-like character of expelled oils with uranium content (Fig. 10) may be explained by radiation-initiated polymerization in the kerogens. CHARLESBY (1954) has shown that high-energy radiation initiates crosslinking in *n*-alkanes and long-chain polymers through a free-radical mechanism. The reaction is initiated by absorption of radiation energy in a hydrocarbon chain, resulting in the loss of a hydrogen atom to form a free radical. Interaction between this free radical and a neighboring chain causes the loss of another hydrogen atom and formation of a cross-linking carbon-carbon bond. This cross-linking increases with increasing radiation dosages until the amount of crosslinking renders *n*-alkanes and long-chain polymers

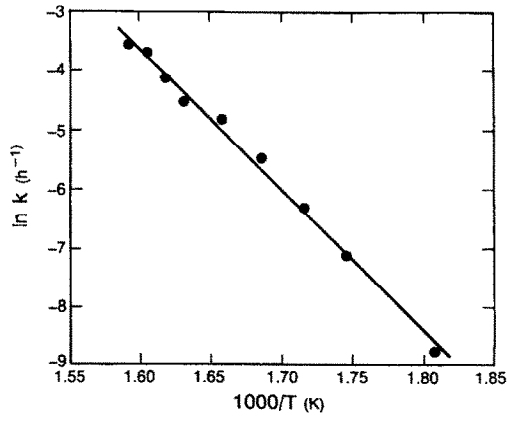


FIG. 11. Arrhenius plot for generation of expelled oil from sample AS-33. The rate constant ($k$) is based on the first-order rate law, $k = [1n(1/\{1 - X\})]1/t$ where $t$ is the duration of the experiment and $X$ is the decimal fraction of expelled oil generated. The regression line is expressed as $1nk = -24208(1/T) + 35.11$ with a correlation coefficient of −0.997.

Table 9. Comparison of Oil Generation Kinetics and Kerogen Compositions of Phosphoria Retort Shale, Alum Shale, and Woodford Shale

| | Phosphoria Retort Shale* | Alum Shale | Woodford Shale* |
|---|---|---|---|
| KINETIC PARAMETERS | | | |
| Activation Energy ($kJmol^{-1}$) | 178.69 | 201.26 | 218.25 |
| Pre-Exponential Factor ($hr^{-1}$) | $4.92 \times 10^{13}$ | $1.77 \times 10^{15}$ | $6.51 \times 10^{16}$ |
| KEROGEN COMPOSITION | | | |
| Carbon (wt.%) | 74.5 | 76.2 | 78.2 |
| Hydrogen (wt.%) | 7.5 | 7.1 | 7.7 |
| Oxygen (wt.%) | 6.2 | 7.5 | 7.0 |
| Nitrogen (wt.%) | 2.8 | 1.7 | 2.1 |
| Sulfur (wt.%)** | 9.0 | 7.4 | 5.0 |
| H/(C+H) | 0.547 | 0.523 | 0.542 |
| O/(C+O) | 0.059 | 0.068 | 0.063 |
| N/(C+N) | 0.031 | 0.018 | 0.023 |
| S/(C+S) | 0.043 | 0.035 | 0.023 |
| $\delta^{13}C$ (PDB) | -29.3 | -29.2 | -29.6 |

* Data from Lewan (1985).

** Values are of organic sulfur and do not include sulfur in the form of iron sulfides.

infusible. The radiation dosage required to reach this infusible state diminishes exponentially with increasing chain length as shown in Fig. 12. This relationship suggests that the increase in condensate-like character of expelled oils with increasing uranium content (Fig. 10) may be attributed to radiation-induced cross-linking of longer n-alkane precursors in the kerogen matrix.

Contrary to oil maturation trends in laboratory experiments and the natural system, the expelled oils from sample AS-33 become less condensate-like with increasing thermal stress (Table 8). This reversal suggests that some *n*-alkanes with a minimal amount of crosslinking are released from the kerogen matrix at higher thermal stresses. This delayed generation of *n*-alkanes appears to end at the end of primary oil generation with an $n\text{-}C_{11}$ index of 17.37 after 72 hours at 360°C (Table 8). At higher thermal stress levels, the usual thermal degradation of *n*-alkanes resulting in an increase in condensate-like character of the oil is expected. This is demonstrated by the expelled oil generated at 365°C after 72 hours showing a slight increase in the $n\text{-}C_{11}$ index (Table 8). In addition to *n*-alkane precursors, branched- and cyclic-alkane components in the kerogen matrix are also susceptible to radiation-induced polymerization. As the intensity of crosslinking increases, the amount of kerogen susceptible to thermal decomposition into oil is expected to decrease. This is shown in Fig. 8 by the negative relationship between uranium content and amount of expelled oil generated at 340°C after 72 hours. These expelled-oil yields do not represent maximum yields, and therefore, some of the variation may be due to inherent differences in the oil-generation kinetics of the samples (LEWAN, 1985). Although radiation damage has reduced the oil-generation potential of the Alum Shale, its overall kinetics for oil generation remain comparable to other source rocks containing type-II kerogens (Table 9).

The proportionality of hydrogen to carbon decreases with increasing crosslinking as a result of the loss of two hydrogens for each crosslinking bond. CHARLESBY (1954) showed a linear decrease in the atomic H/C ratio of polyethylene from 1.99 to 1.68 with increasing radiation dosage. This is also observed in the Alum Shale with atomic H/C ratios of the kerogens decreasing linearly from 1.16 to 1.01 with increasing uranium content (Fig. 2a). Concern that this decrease in the atomic H/C ratios is a result of variations in the amount of thermal stress experienced by the samples may be dismissed by the positive correlation between this ratio and the bitumen/organic carbon ratio. Thermal maturation of organic matter initially involves the breakdown of kerogen to bitumen (LEWAN, 1985). This process results in a decrease in the kerogen H/C ratio and an increase in the bitumen/organic carbon ratio (TISSOT and WELTE, 1978, pp. 467–468), which is contrary to the relationship observed in the Alum Shale (Fig. 2).

The decrease in bitumen/organic carbon ratios with increasing uranium content (Fig. 2b) is also attributed to radiation-induced cross-linking. It is envisaged that the extractable bitumen represents portions of original bitumen that has not incurred radiation-induced crosslinking as a result of its proximity to the uranium in the rock. This interpretation suggests that the *n*-alkane, acyclic isoprenoid, and sterane distributions are representative of the original bitumen. Conversely, hopanes and triaromatic steroid hydrocarbons do appear to have been affected by radiation. An explanation for this discrimination is not apparent, but it suggests the composition of bitumen is not uniformly distributed throughout the rock.

*Alteration of biological markers:* The ratio of the 20S and 20R isomers of 24-ethyl-14$\alpha$, 17$\alpha$-cholestane ($\alpha\alpha$C29) has been shown to be sensitive to thermal stress with a maximum equilibrium ratio of 0.56 (*i.e.*, 20S/[20R + 20S]) occurring at vitrinite reflectance values less than 1.25% $R_0$ (MACKENZIE, 1984). Although reversals in this ratio at higher levels of thermal stress complicate its interpretation (LEWAN *et al.*, 1986), reflectance values and atomic H/C ratios corroborate the thermal immaturity indicated by the low isomer ratios (Table 7). The sensitivity of this ratio to thermal stress (MACKENZIE and MCKENZIE, 1983; SUZUKI, 1984) and the lack of a significant correlation between it and uranium content indicate

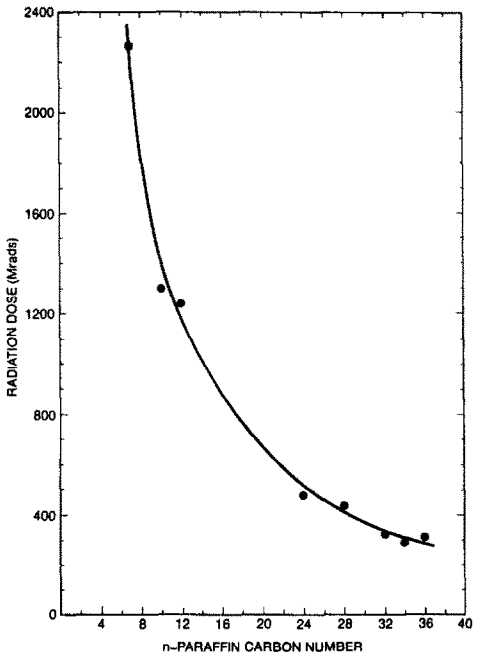


FIG. 12. Radiation dosage required to render normal alkanes infusible (CHARLESBY, 1960).

radiogenic heat has had a negligible effect on these rocks. Although radiogenic heat from a sedimentary sequence several kilometers thick may be an important consideration in reconstructing thermal histories (KEEN and LEWIS, 1982), the thin character of the Alum Shale (<25 m) and its uranium-enriched zones (<10 m) reduces the significance of its radiogenic heat. Calculations in Appendix I show that radiogenic heat from a 10-m thick Alum Shale with a 440 ppm uranium content increases normal thermal gradients by only 1.3 percent. This amounts to a temperature increase of only a few degrees at burial depths of several kilometers.

Reduction of the $C_{26}$ through $C_{28}$ triaromatic steroids relative to the $C_{20}$ and $C_{21}$ triaromatic steroids with increasing thermal stress has been well documented (MACKENZIE *et al.*, 1981; SHI JI-YANG *et al.*, 1982; SCHOU *et al.*, 1984; LEWAN *et al.*, 1986). Although this relative change is usually attributed to cleavage of the longer side chains, it may also be attributed to assimilation of triaromatics with longer side chains into the kerogen matrix. The latter best explains the relationship in the Alum Shale between changes in the triaromatic-steroid distribution and uranium content (Fig. 7a), with radiation-induced polymerization favoring the longer side chains. In addition, the preferential decrease in the $C_{28}$ triaromatics with the overall decrease in $C_{26}$ through $C_{28}$ triaromatic steroids (Fig. 7b) may be explained by the greater susceptibility of branched alkanes to radiation induced polymerization (CHARLESBY, 1960, p. 210). This preferential loss of $C_{28}$ triaromatics is not observed in thermal maturity sequences and may serve as a means of distinguishing between the effects of radiation damage and thermal stress.

Similar to the $\alpha\alpha C_{29}$ sterane isomer ratio, the hopane Ts/Tm ratio of the Alum Shale indicates thermal immaturity. But unlike the sterane isomer ratio, the variations in the Ts/Tm ratio have a strong positive correlation with uranium content ($r = 0.949$). This relationship is difficult to explain as a result of radiation-induced polymerization because of structural similarities of the two $C_{27}$ triterpanes and their lack of alkyl side chains. One possible explanation is that tetracyclic or tricyclic terpanes with strong m/z 191 fragments coelute with the Ts or Tm peaks as noted by SEIFERT and MOLDOWAN (1986). Coelution of the Tm peak with a tetracyclic terpane bearing a long alkyl side chain would cause an apparent increase in the Ts/Tm ratio as radiation-induced polymerization of the side chain reduces the concentration of the coeluting terpane. This possibility is supported by the observation that a $C_{30}$ tetracyclic triterpane coelutes with the Tm peak in some crude oils (VOLKMAN *et al.*, 1983).

*Kerogen properties not affected:* Higher reflectivities of vitrinites from coals and coalified logs associated with high uranium concentrations have been well documented (TEICHMÜLLER and TEICHMÜLLER, 1958; ERGUN *et al.*, 1960; JEDWAB, 1966; GENTRY *et al.*, 1976; and SASSEN, 1983). These higher reflectivities usually occur as localized halos or bands around uranium minerals within the coals or coalified logs. SASSEN (1983) observed Jurassic coalified logs with uranium concentrations less than 55,000 ppm having unaltered mean vitrinite reflectance values between 0.41 and 0.54% $R_0$, and those with uranium concentrations in the range of 150,000 to 195,000 ppm having altered mean vitrinite-reflectance values between 0.63 and 0.82% $R_0$. These uranium concentrations are more than two-orders of magnitude greater than those of the Alum Shale samples, and therefore, it is not surprising that no relationship was observed between uranium content and reflectance of the vitrinite-like macerals.

Variations in the stable carbon isotopes (*i.e.*, $\delta^{13}C$) of the Alum Shale kerogens do not correlate with variations in the uranium contents of the rocks. This does not support the interpretation by LEVENTHAL and THRELKELD (1978) on radiation-induced isotope fractionation of organic matter in Jurassic sandstones. Their interpretation is based on the $\delta^{13}C$ of organic matter in a high-grade ore (U = 3,900 to 28,700 ppm) having a 5 to 8 per mil heavier value relative to the organic matter in adjacent lower-grade ores (U = 80 to 380 ppm). A major assumption in this interpretation is that the organic matter in the high- and low-grade ores originally had similar isotopic compositions. The strong bimodal distribution of organic carbon contents, with the high-grade ore containing as much as 5.0 wt% organic carbon and the low-grade ore containing only 0.2 or less wt% organic carbon, makes this assumption questionable. A study by HATCHER *et al.* (1986) on uranium-associated organic matter in the Jurassic Morrison Formation has also questioned this assumption. In addition, radiation-induced isotope fractionation has not been observed in the Cluff Lake uranium deposit (LEVENTHAL *et al.*, 1987) nor in the uraniferous organic-rich nodules of southwestern Oklahoma (CURIALE *et al.*, 1983).

*Radiation dosage:* The radiation dosage experienced by organic matter in the Alum Shale samples is difficult to assess without knowing the spatial distribution of uranium relative to the disseminated organic matter. Uranium in black shales usually occurs in submicron domains associated with organic matter, as well as sequestered in mineral phases (ROSS, 1952; BATES and STRAHL, 1957; RYNNINGER, 1957). Although available data in this study does not permit determination of the mean distance between uranium domains and organic matter in each sample, it does permit determination of a maximum possible dosage for each sample. The amount of energy emitted ($Q$) in MeV units from the decay series of $^{235}U$ and $^{238}U$ in 100 grams of rock is determined by the expression

$$Q = \bar{U}_t\left[\frac{1.1905 \times 10^{23}}{\exp\{-1.55 \times 10^{-10}\Delta t\}} + \frac{8.3304 \times 10^{20}}{\exp\{-9.8485 \times 10^{-10}\Delta t\}} - 1.1988 \times 10^{23}\right] \quad (1)$$

where $\bar{U}_t$ is the present-day weight percent uranium content of a rock, and $\Delta t$ is the age of the rock in Ma b.p. Derivation of this equation and its inclusive constants are given in Appendix II. Using this equation, the amount of radiation energy emitted within 100 g of rock over 500 Ma is tabulated for each sample in Table 10. A maximum possible dosage experienced by the organic matter is determined by assuming all the emitted radiation energy ($Q$) is absorbed by the organic matter. This is calculated by converting $Q$ from MeV to ergs (*i.e.*, 1 MeV = $1.602 \cdot 10^{-6}$ ergs), and dividing it by the weight percent of organic carbon. The quotient is converted to Mrads (*i.e.*, $1 \cdot 10^8$ ergs/g = 1 Mrad), and the resulting maximum possible dosage for each sample is given in Table 10. These

Table 10. Radiation Energy Emitted Over the Last 500 Ma from the Decay of $^{238}U$ and $^{235}U$ in Thermally Immature Samples of Alum Shale

| Sample Number | Present Day Uranium Content of Rock ($\bar{U}_t$; wt.% x $10^4$) | Radiation Energy Emitted per 100 g of Rock (Q; MeV/100g rock x $10^{-20}$) | Maximum Possible Dosage (ergs/g Org.C x $10^{-13}$ or Mrads in Org.C x $10^{-5}$) |
|---|---|---|---|
| BB-8681 | 18 | 0.18225 | 0.3395 |
| AS-40 | 60 | 0.60749 | 1.0137 |
| F-2255 | 110 | 1.11373 | 1.7322 |
| BB-8703 | 120 | 1.21497 | 1.1122 |
| BB-8701 | 130 | 1.31622 | 1.7005 |
| AS-33 | 150 | 1.51872 | 1.8432 |
| AS-8 | 180 | 1.82246 | 1.5954 |
| BB-8707 | 180 | 1.82246 | 1.5954 |
| AS-31 | 190 | 1.92371 | 1.3341 |
| AS-34 | 190 | 1.92371 | 2.5897 |
| BB-8706 | 260 | 2.63245 | 2.1964 |
| BB-8702 | 370 | 3.74617 | 3.8225 |
| J-6222 | 380 | 3.84742 | 3.1608 |
| BB-8705 | 420 | 4.25241 | 3.5667 |
| AS-32 | 440 | 4.45491 | 3.9648 |

dosages are expressed with respect to organic carbon rather than organic matter to facilitate comparisons with other published data, which usually give only the former.

The maximum possible dosages in Table 10 are at least one order of magnitude greater than the dosages required to make $n$-$C_{12}$ infusible ($1.24 \cdot 10^3$ Mrads; CHARLESBY, 1960, p. 209), crude oils heavier and more viscous ($10^3$ Mrads; COLOMBO *et al.*, 1964; CARROLL and BOLT, 1963), polyethylene insoluble ($4 \cdot 10^2$ Mrads; CHARLESBY, 1960, p. 210), and natural rubber brittle ($10^3$ Mrads; SISMAN *et al.*, 1963). Approximately 90% of the maximum possible dosage is a result of $\alpha$ decay, with the remaining radiation being mostly a result of $\beta$ decay. Although equivalent dosages from different radiation sources cause essentially the same amount and type of damage (CHARLESBY, 1960, p. 7; CHAPIRO, 1962, p. 227), appreciable variations in the penetration power of the different radiation sources does put some constraints on their effectiveness within a rock. $\alpha$ radiation within a rock only penetrates a few tens of microns, which limits its effectiveness to uranium domains in direct contact with organic matter. $\beta$ and $\gamma$ radiation within a rock is more penetrative with distances in the range of millimeters and centimeters, respectively. These are expected to be more effective where uranium is not in intimate contact with the organic matter, and ten percent of the maximum possible dosages in Table 10 is still sufficient to account for the observed damage.

Samples BB-8681 and AS-40 have the lowest maximum possible dosages (Table 10), and with respect to their kerogen H/C ratios (Fig. 2a), bitumen/organic carbon ratios (Fig. 2b), hopane abundances (Table 7), triaromatic steroid ratios (Fig. 7a), and expelled pyrolysate $n$-$C_{11}$ indices (Fig. 10) have no obvious signs of radiation damage. The likelihood of radiation damage to organic matter in black shales of different geological ages may be approximated by using the larger of these two maximum possible dosages as a threshold value for $Q$ (*i.e.*, $1.0137 \cdot 10^5$ Mrads = $6.328 \cdot 10^{18}$ MeV/g org.C) in Eqn. (1). This is shown graphically in Fig. 13 with respect to geological age and uranium/organic carbon ratio. The potential for notable radiation damage to thermally immature organic matter in black shales is low for those that plot above the curve and high for those that plot below the curve. Use of this approximation should *not* be extended to phosphorites or limestones because of the high proportion of uranium that is usually sequestered in mineral grains (MCSWIGGEN *et al.*, 1986; DEGENS *et al.*, 1977). This reduces the effectiveness of the maximum possible dosage, and the curve in Fig. 13 is expected to shift to higher $\bar{U}_t$/org.C ratios for these lithologies. Black shales are defined here as very-fine grained sedimentary rocks (LEWAN, 1978) with organic carbon contents greater than 2 weight percent (BELL, 1978).

Available data on black shales of different ages are plotted for comparison in Fig. 13. The data indicate that there is a low potential for radiation damage in most Phanerozoic black shales, particularly those of Mesozoic and Cenozoic ages. Paleozoic black shales also have a low potential for radiation damage, but the Alum Shale and Schaentzel shales are notable exceptions. No data is presented on Precambrian black shales, but the radiation-damage curve in Fig. 13 intercepts the $\bar{U}_t$/org.C ratio of one at 2445 Ma. Black shales of this age or older with $\bar{U}_t$/org.C ratios within the range of the Cenozoic and Mesozoic black shales will have a high potential for radiation damage. Unfortunately, documenting radiation

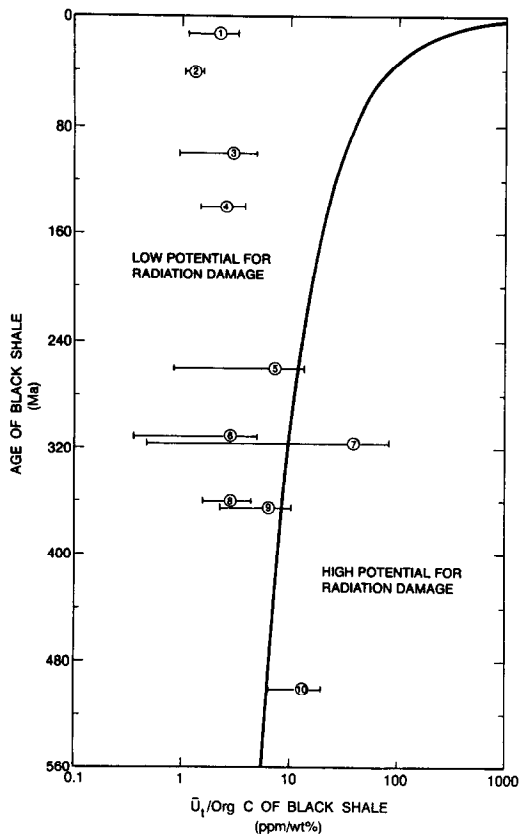


FIG. 13. Relationship between age and $\bar{U}_t$/org.C ratio of black shales for determining high and low potentials for radiation damage to organic matter. Black shales plotted on diagram include: (1) twenty-eight samples of Monterey Shale from Naples, California; (2) five samples of Kreyenhagen Shale from Kings and Fresno Counties, California; (3) eighteen samples of Mowry Shale from Wyoming and Utah; (4) seven samples of the Janusfjellet Formation (DYPVIK and BUE, 1984); (5) forty-five samples of Phosphoria shale from southwestern Montana (CRESSMAN and SWANSON, 1964); (6) eleven samples of Excello Shale (JAMES, 1970); (7) twenty-eight samples of Schaentzel shale from France (BATES *et al.*, 1956); (8) thirteen samples of Ohio Shale (LEVENTHAL, 1981); (9) sixteen samples of Woodford Shale (OLSON, 1982); (10) fourteen samples of Alum Shale. Circles designate mean values and bars designate standard deviations.

damage in black shales of Archean age is hindered by the rarity of thermally immature rocks of this age (HAYES *et al.*, 1983, Fig. 5-9). Once thermal maturation of a black shale commences, the effects of radiation damage are expected to be minimized. This is a result of the increase in aromatization of organic matter with increasing thermal stress (BÉHAR and VANDENBROUCKE, 1986) and the highly resistant nature of aromatic hydrocarbons to radiation (CHARLESBY, 1960, p. 192; CARROLL and BOLT, 1963).

## CONCLUSIONS

The anomalously high concentrations of syngenetic or early diagenetic uranium in thermally immature Alum Shale provides a unique opportunity to study the effects of radiation on organic matter over approximately a 500 Ma time interval. Generation of condensate-like oils at reduced yields by hydrous pyrolysis (340°C/72h) from samples with high uranium concentrations (>100 ppm) is one of the most obvious results of radiation damage. This is explained by radiation-induced cross-linking of normal alkanes through a free-radical mechanism, which at a critical radiation dosage renders the alkanes infusible and insoluble. The critical dosage decreases exponentially as chain length increases, and explains the increase in condensate-like character and reduced yields of expelled oil with increasing uranium content. Although radiation affects the yield and alkane composition of the expelled oils, it does not alter the overall kinetics for oil generation.

Additional consequences of the radiation-induced cross-linking are reductions in atomic H/C ratios of the kerogens and bitumen/organic-carbon ratios of the rocks with increasing uranium content. Low 20S/20R isomer ratios of the $\alpha\alpha C_{29}$ sterane and their lack of a significant correlation with uranium content suggests that the amount of radiogenic heat produced had a negligible effect on these thermally immature rocks. Triaromatic-steroid distributions in the m/z 231 ion chromatograms show an increase in $C_{20}$ and $C_{21}$ and a decrease in $C_{28}$ relative to $C_{26}$ and $C_{27}$ with increasing uranium content. Although the former change in the distribution is indicative of thermal maturation, the latter change in the distribution is not. Both changes in distribution are attributed to radiation-induced crosslinking of the longer side chains on the $C_{26}$ through $C_{28}$ structures, with the branched side chain on the $C_{28}$ structure being the most susceptible.

Radiation-induced isotope fractionation was not observed in $\delta^{13}C$ values of the kerogens. The major effect of radiation on the organic matter appears to have been polymerization through crosslinking, rather than fragmentation through chain scission. Dominance of the former process makes significant fractionation of $\delta^{13}C$ unlikely. Reflectance measurements on vitrinite-like macerals showed no covariance with uranium content. Changes in vitrinite reflectance have been observed in epigenetic uranium ore deposits, but in these deposits the uranium concentrations are several orders of magnitude greater than those in the Alum Shale.

The radiation dosage necessary to facilitate radiation damage to organic matter similar to that observed in the Alum Shale has been estimated to be $1.0173 \cdot 10^5$ Mrads with respect to organic carbon. This estimate does not take into account the spatial distribution of uranium relative to the organic matter nor the sequestering of uranium in minerals. The estimate is approximately two orders of magnitude greater than dosages measured in the laboratory for alteration of organic matter. This estimate may be used to evaluate the potential of radiation damage to thermally immature black shales throughout the geological rock record.

*Acknowledgements*—The authors thank Amoco Production Company for supporting this research and permission to publish it. Valuable laboratory assistance was provided by V. L. Marshall, J. D. Redding, R. C. Robinson and F. Vu from the Amoco Production Company Research Center, and valuable field assistance was provided by T. Dons, B. Jensen and M. Olsen from the University of Copenhagen. Critical reviews of the manuscript by D. L. Dolcater, T. Eglington, J. S. Leventhal, G. Lijmbach, B. E. Torkelson, J. A. Williams, and J. C. Winters are appreciated.

*Editorial handling:* J. W. de Leeuw

## REFERENCES

ANDERSSON A., DAHLMAN B. and GEE D. (1983) Kerogen and uranium resources in the Cambrian Alum Shale of the Billingen-Falbygden and Närke areas, Sweden. *Geol. Fören. Stockh. Förh.* **104,** 197–209.

ANDERSSON A., DAHLMAN B., GEE D. and SNÄLL S. (1985) The Scandinavian Alum Shales. *Sver. Geol. Unders. Ser.* Ca 56, Uppsala, 50p.

ARMANDS G. (1972) Geochemical studies of uranium, molybdenium and vanadium in a Swedish Alum Shale. *Stockh. Contr. Geol.* **27,** 1–148.

BANKS H. P. (1975) Early vascular land plants: proof and conjecture. *BioScience* **25,** 730–737.

BATES T. F. and STRAHL E. O. (1957) Mineralogy, petrography, and radioactivity of representative samples of Chattanooga Shale. *Geol. Soc. Amer. Bull.* **68,** 1305–1314.

BATES T. F. and STRAHL E. O. (1958) Mineralogy and chemistry of uranium-bearing black shales. In *Proc. 2nd United Nations Intl. Conf. Peaceful Uses of Atomic Energy,* vol. 2, pp. 407–411.

BATES T. F., WRIGHT H. D., STRAHL E. O., STANONIS F. L., SILVERMAN E. N., O'NEIL R. L., GRACE J. D., DUEY H. D., DOLSEN C. P. and BUCKWOLD S. J. (1956) An investigation of the mineralogy, petrography, and paleobotany of uranium-bearing shales and lignites. *Fifth Ann. Rept. U.S. Atomic Energy Comm., NYO-7411.*

BEHAR F. and VANDENBROUCKE M. (1986) Représentation chimique de la structure des kérogénes et des asphaltènes en fonction de leur origine et de leur degré d'evolution. *Rev. l'Inst. Franc. Pétrole* **41,** 173–188.

BELL R. T. (1978) Uranium in black shales—a review. In *Uranium Deposits, Their Mineralogy and Origin* (ed. M. M. KIMERBLY); *Mineral. Assoc. Can. Short Course Handbk. 3,* pp. 307–329.

BIRCH F. (1954) Heat from radioactivity. In *Nuclear Geology* (ed. H. FAUL), pp. 148–174. J. Wiley & Sons, New York.

BREGER I. A. (1974) The organic geochemistry of the coal-uranium association. In *Intl. Atomic Energy Agency, Vienna, SM-183/29,* pp. 99–124.

BREGER I. A. and BROWN A. (1963) Distribution and types of organic matter in a barred marine basin. *Trans. N.Y. Acad. Sci.* **25,** 741–755.

BRYHNI I. and BRASTAD K. (1980) Caledonian regional metamorphism in Norway. *J. Geol. Soc. London* **137,** 251–260.

BUCHARDT B. and LEWAN M. D. (1989) Reflectance of vitrinite-like macerals as a thermal maturity index in the Cambro-Ordovician Alum Shale of southern Scandinavia. *Amer. Assoc. Petrol. Geol. Bull.* (submitted).

BUCHARDT B., CLAUSEN J. and THOMSEN E. (1986) Carbon isotope composition of Lower Palaeozoic kerogen: Effects of maturation. *Org. Geochem.* **10,** 127–134.

CAMERON E. M. and GARRELS R. M. (1980) Geochemical compositions of some Precambrian shales from the Canadian Shield. *Chem. Geol.* **28,** 181–197.

CARROLL J. G. and BOLT R. O. (1963) Lubricants. In *Radiation Effects on Organic Materials* (eds. R. O. BOLT and J. G. CARROLL), pp. 349–406. Academic Press, London.

CHAPIRO A. (1962) *Radiation Chemistry of Polymeric Systems*. J. Wiley & Sons, New York.

CHARLESBY A. (1954) The cross-linking and degradation of paraffin chains by high-energy radiation. *Proc. Roy. Soc. London* **A222**, 60–74.

CHARLESBY A. (1960) *Atomic Radiation and Polymers*. Pergamon Press, New York.

CLARKE F. W. (1924) Data of geochemistry. *U.S. Geol. Surv. Bull. 770*, 841p.

COLOMBO U., DENTI E. and SIRONI G. (1964) A geochemical investigation upon the effects of ionizing radiation on hydrocarbons. *J. Inst. Petrol.* **50**, 228–237.

CRESSMAN E. R. and SWANSON R. W. (1964) Stratigraphy and petrology of the Permian rocks of southwestern Montana. *U.S. Geol. Surv. Prof. Pap. 313-C*, 569p.

CROW E. L., DAVIS F. A. and MAXFIELD M. W. (1960) *Statistics Manual*. Dover, New York.

CURIALE J. A., BLOCH S., RAFALSKA-BLOCH J. and HARRISON W. E. (1983) Petroleum related origin for uraniferous organic-rich nodules of southwestern Oklahoma. *Amer. Assoc. Petrol. Geol. Bull.* **67**, 588–608.

DEGENS E. T., KHOO F. and MICHAELIS W. (1977) Uranium anomaly in Black Sea sediments. *Nature* **269**, 566–569.

DYPVIK H. and BUE B. (1984) The U, Th and K distribution in black shales of the Janusfjellet Formation, Svalbard, Norway. *Chem. Geol.* **42**, 287–296.

ECKEL E. C. (1904) On the chemical composition of American shales and roofing slates. *J. Geol.* **12**, 25–29.

ERGUN S., DONALDSON W. F. and BREGER I. A. (1960) Some physical and chemical properties of vitrains associated with uranium. *Fuel* **39**, 71–77.

FAURE G. (1986) *Principles of Isotope Geology*. J. Wiley & Sons, New York.

FROST J. K., ZIERATH D. L. and SHIMP N. F. (1985) Chemical composition and geochemistry of the New Albany Shale Group (Devonian-Mississippian) in Illinois. *Ill. State Geol. Surv. Grant Rept. 1985-4*.

GENTRY R. V., CHRISTIE W. H., SMITH D. H., EMERY J. F., REYNOLDS S. A., WALKER R., CRISTY S. S. and GENTRY P. A. (1976) Radiohalos in coalified wood: New evidence relating to the time of uranium introduction and coalification. *Science* **194**, 315–318.

GROMET L. P., DYMEK R. F., HASKIN L. A. and KOROTEV R. L. (1984) The "North American Shale Composite": Its compilation, major and trace element characteristics. *Geochim. Cosmochim. Acta* **48**, 2469–2482.

HARRELL J. A. (1984) *Bivariate Regression and Correlation Analyses in Geology*. Short Course Notes, 2nd Ann. Combined Meeting Ohio and Michigan Sections, Amer. Inst. Prof. Geol., Toledo.

HARRELL J. A. (1987) The analysis of bivariate association. In *Use and Abuse of Statistical Methods in the Earth Sciences* (ed. W. B. SIZE), pp. 142–165. Oxford Univ. Press, New York.

HARWOOD R. J. (1977) Oil and gas generation by laboratory pyrolysis of kerogen. *Amer. Assoc. Petrol. Geol. Bull.* **61**, 2082–2102.

HATCHER P. G., SPIKER E. C., OREM W. H., ROMANKIW L. A., SZEVERENYL N. M. and MACIEL G. E. (1986) Organic geochemical studies of uranium-associated organic matter from the San Juan Basin: A new approach using solid-state $^{13}C$ nuclear magnetic resonance. In *A Basin Analysis Case Study: The Morrison Formation, Grants Uranium Region, New Mexico* (eds. C. E. TURNER-PETERSON and E. S. SANTOS); *Amer. Assoc. Petrol. Geol. Studies in Geology 22*, pp. 171–184.

TEN HAVEN H. L., DE LEEUW J. W. and SCHENCK P. A. (1985) Organic geochemical studies of a Messinian evaporitic basin, northern Apennines (Italy): I. Hydrocarbon biological markers for a hypersaline environment. *Geochim. Cosmochim. Acta* **49**, 2181–2191.

HAYES J. M., KAPLAN I. R. and WEDEKING K. W. (1983) Precambrian organic geochemistry, preservation of the record. In *Earth's Earliest Biosphere* (ed. J. W. SCHOPF), pp. 93–134. Princeton Univ. Press, Princeton, NJ.

HOERING T. C. and NAVALE V. (1987) A search for molecular fossils in the kerogen of Precambrian sedimentary rocks. *Precamb. Res.* **34**, 247–267.

HUGHES W. B., HOLBA A. G., MILLER D. E. and RICHARDSON J. S. (1985) Geochemistry of Greater Ekofisk crude oils. In *Petroleum Geochemistry in Exploration of the Norwegian Shelf* (ed. B. M. THOMAS), pp. 75–92. Graham & Trotman, London.

JAFFEY A. H., FLYNN K. F., GLENDENIN L. E., BENTLEY W. C. and ESSLING A. M. (1971) Precision measurement of half-lives and specific activities of $^{235}U$ and $^{238}U$. *Physical Review* **C**, 1889–1906.

JAMES G. W. (1970) Stratigraphic geochemistry of a Pennsylvanian black shale (Excello) in the Mid-Continent and Illinois Basin. Ph.D. dissertation, Rice University, Houston.

JEDWAB J. (1966) Les dégâts radiatifs dans le charbon uranifère du Schaentzel. *Geologische Rund.* **55**, 445–453.

JIAMO F., GUOYING S., PINGAN P., BRASSELL S. C., EGLINTON G. and JIGANG J. (1985) Pecularities of Salt Lake sediments as potential source rocks in China. *Org. Geochem.* **10**, 119–126.

KEEN C. E. and LEWIS T. (1982) Measured radiogenic heat production in sediments from continental margin of eastern North America: Implications for petroleum generation. *Amer. Assoc. Petrol. Geol. Bull.* **66**, 1402–1407.

KEITH M. L. and DEGENS E. T. (1959) Geochemical indicators of marine and fresh-water sediments. In *Researches in Geochemistry* (ed. P. H. ABELSON), pp. 38–61. J. Wiley & Sons, New York.

KISCH H. J. (1980) Incipient metamorphism of Cambro-Silurian clastic rocks from the Jämtland Supergroup, central Scandinavian Caledonides, western Sweden: Illite crystallinity and "vitrinite" reflectance. *J. Geol. Soc. London* **137**, 271–288.

KRISTIANSEN J., SAXOV S., BALLING N. and POULSEN K. (1982) *In-situ* thermal conductivity measurements of Precambrian, Paleozoic and Mesozoic rocks on Bornholm, Denmark. *Geol. Fören. Stockh. Förh* **104**, 49–56.

LEE W. H. K. (1963) Heat flow data analysis. *Rev. Geophysics* **1**, 449–479.

LEVENTHAL J. S. (1981) Pyrolysis gas chromatography-mass spectrometry to characterize organic matter and its relationship to uranium content of Appalachian Devonian black shales. *Geochim. Cosmochim. Acta* **45**, 883–889.

LEVENTHAL J. S., GRAUCH R. I., THRELKELD C. N., LICHTE F. E. and HARPER C. T. (1987) Unusual organic matter associated with uranium from the Claude Deposit, Cluff Lake, Canada. *Econ. Geol.* **82**, 1169–1176.

LEVENTHAL J. S. and THRELKELD C. N. (1978) Carbon-13/carbon-12 isotope fractionation of organic matter associated with uranium ores induced by alpha irradiation. *Science* **202**, 430–432.

LEWAN M. D. (1978) Laboratory Classification of very fine-grained sedimentary rocks. *Geology* **6**, 745–748.

LEWAN M. D. (1980) Geochemistry of vanadium and nickel in organic matter of sedimentary rocks. Ph.D. dissertation, Univ. Cincinnati.

LEWAN M. D. (1983) Effect of thermal maturation on stable organic carbon isotopes as determined by hydrous pyrolysis of Woodford Shale. *Geochim. Cosmochim. Acta* **47**, 1471–1479.

LEWAN M. D. (1985) Evaluation of petroleum generation by hydrous pyrolysis experiments. *Phil. Trans. Roy. Soc. London* **A312**, 123–134.

LEWAN M. D. (1986) Stable carbon isotopes of amorphous kerogens from Phanerozoic sedimentary rocks. *Geochim. Cosmochim. Acta* **50**, 1583–1591.

LEWAN M. D. (1987) Petrographic study of primary petroleum migration in the Woodford Shale and related rock units. In *Migration of Hydrocarbons in Sedimentary Basins* (ed. B. DOLIGEZ), pp. 113–130. I.F.P., Editions Technip, Paris.

LEWAN M. D., BJORØY M. and DOLCATER D. L. (1986) Effects of thermal maturation on steroid hydrocarbons as determined by hydrous pyrolysis of Phosphoria Retort Shale. *Geochim. Cosmochim. Acta* **50**, 1977–1987.

LIJMBACH G. W. M. (1975) On the origin of petroleum. *9th World Petrol. Congress Proc.* **2**, 357–369.

MACKENZIE A. S. (1984) Applications of biological markers in petroleum geochemistry. In *Advances in Petroleum Geochemistry* (eds., J. BROOKS and D. WELTE), pp. 115–214. Academic Press, London.

MACKENZIE A. S. and MCKENZIE D. (1983) Isomerization and aromatiziation of hydrocarbons in sedimentary basins formed by extension. *Geol. Mag.* **120,** 417–528.

MACKENZIE A. S., HOFFMANN C. F. and MAXWELL J. R. (1981) Molecular parameters of maturation in the Toarcian Shales, Paris Basin, France—III. Changes in aromatic steroid hydrocarbons. *Geochim. Cosmochim. Acta* **45,** 1345–1355.

MCLENNAN S. M. and TAYLOR S. R. (1983) Geochemical evolution of Archean shales from South Africa. I. The Swaziland and Pongola Supergroups. *Precam. Res.* **22,** 93–124.

MCSWIGGEN P. L., MOREY G. B. and WEIBLEN P. W. (1986) Uranium in early Proterozoic phosphate-rich metasedimentary rocks of east-central Minnesota. *Econ. Geol.* **81,** 173–183.

NANZ R. H., JR. (1953) Chemical composition of Precambrian slates with notes on the geochemical evolution of lutites. *J. Geol.* **61,** 51–64.

OLSON R. K. (1982) Factors controlling uranium distribution in Upper Devonian—Lower Mississippian black shales of Oklahoma and Kansas. Ph.D. dissertation, Univ. Tulsa.

PEARSON M. J. (1979) Geochemistry of the Hepworth Carboniferous sediment sequence and origin of the diagenetic iron minerals and concretions. *Geochim. Cosmochim. Acta* **43,** 927–941.

PIERCE A. P., MYTTON J. W. and BARNETT P. R. (1958) Geochemistry of uranium in organic substances in petroliferous rocks. In *Proc. 2nd. United Nations Intl. Conf. Peaceful Uses of Atomic Energy,* vol. 2, pp. 192–198.

PRIEM H. N. A., MULDER F. G., BOELRIJK N. A. I. M., HEBEDA F. H., VERSCHURE R. H. and VERDURMEN E. A. T. H. (1968) Geochronological and palaeomagnetical reconnaissance survey in part of central and southern Sweden. *Phys. Earth Planet. Interiors* **1,** 373–380.

RONOV A. B. and MIGDISOV A. A. (1971) Geochemical history of the crystalline basement and the sedimentary cover of the Russian and North American Platforms. *Sedimentology* **16,** 137–185.

ROSS V. F. (1952) Autoradiographic study of marine shales. *Econ. Geol.* **47,** 783–793.

RYNNINGER R. (1957) Mode of occurrence of uranium in Swedish black shales preliminary investigation. *Geol. Foren. I Stockholm. Forhan.* **79,** 88–90.

SASSEN R. (1983) Increased vitrinite reflectance associated with uranium mineralization. In *Advances in Organic Geochemistry* (ed. M. BJORØY), pp. 94–98. J. Wiley & Sons.

SCHOU L., MØRK A. and BJORØY M. (1984) Correlation of source rocks and migrated hydrocarbons by GC-MS in the Middle Triassic of Svalbard. *Org. Geochem.* **6,** 513–520.

SEIFERT W. K. and MOLDOWAN J. M. (1978) Applications of steranes, terpanes, and monoaromatics to the maturation, migration and source of crude oils. *Geochim. Cosmochim. Acta* **42,** 77–95.

SEIFERT W. K. and MOLDOWAN J. M. (1986) Use of biological markers in petroleum exploration. In *Biological Markers in the Sedimentary Record* (ed., R. B. JOHNS), pp. 261–290. Elsevier, Amsterdam.

SHAW D. M. (1956) Geochemistry of pelitic rocks. Part III: Major elements and general geochemistry. *Geol. Soc. Amer. Bull.* **67,** 919–934.

SHEPPARD C. W. (1944) Radioactivity and petroleum genesis. *Amer. Assoc. Petrol. Geol. Bull.* **28,** 924–952.

SHI JI-YANG, MACKENZIE A. S., ALEXANDER R., EGLINTON G., GOWAR A. P., WOLFF G. A. and MAXWELL J. R. (1982) A biological marker investigation of petroleums and shales from the Shengli oil field, The People's Republic of China. *Chem. Geol.* **35,** 1–31.

SIKANDER A. H. and PITTON J. L. (1978) Reflectance studies on organic matter in Lower Paleozoic sediments of Quebec. *Bull. Can. Petrol. Geol.* **26,** 132–151.

SISMAN O., PARKINSON W. W. and BOPP D. (1963) Polymers. In *Radiation Effects on Organic Materials* (eds. R. O. BOLT and J. G. CARROLL), pp. 127–181. Academic Press, London.

SPEARS D. A. and AMIN M. A. (1981) Geochemistry and mineralogy of marine and nonmarine Namurian black shales from the Tansley borehole, Derbyshire. *Sedimentology* **28,** 407–417.

SPEARS D. A. and SEZGIN H. I. (1985) Mineralogy and geochemistry of the subcrenatum marine band and associated coal-bearing sediments, Langsett, South Yorkshire. *J. Sediment. Petrol.* **55,** 570–578.

SUZUKI N. (1984) Estimation of maximum temperature of mudstone by two kinetic parameters: Epimerization of sterane and hopane. *Geochim. Cosmochim. Acta* **48,** 2273–2282.

SWANSON V. E. (1960) Oil yield and uranium content of black shales. *U.S. Geol. Surv. Prof. Pap. 356-A.*

SWANSON V. E. (1961) Geology and geochemistry of uranium in marine black shales, a review. *U.S. Geol. Surv. Prof. Pap. 356-C.*

TEICHMÜLLER M. and TEICHMÜLLER R. (1958) Inkohlungsuntersuchungen und ihre Nutzanwendung. *Geol. Mijnbouw* **20,** 41–66.

TISSOT B. and WELTE D. H. (1978) *Petroleum Formation and Occurrence.* Springer-Verlag, New York.

TISSOT B., CALIFET-DEBYSER Y., DEROO G. and OUDIN J. L. (1971) Origin and evolution of hydrocarbons in early Toarcian shales, Paris Basin, France. *Amer. Assoc. Petrol. Geol. Bull.* **55,** 2177–2193.

TISSOT B., ESPITALIE J., DEROO G., TEMPERE C. and JONATHAN D. (1974) Origine et migration des hydrocarbures dans le Sahara Oriental (Algerie). In *Advances in Organic Geochemistry 1973* (eds. B. TISSOT and F. BIENNER), pp. 315–334. Editions Technip, Paris.

TUREKIAN K. K. and WEDEPOHL K. H. (1961) Distribution of the elements in some major units of the Earth's crust. *Geol. Soc. Amer. Bull.* **72,** 175–191.

VOLKMAN J. K., ALEXANDER R., KAGI R. I., NOBLE R. A. and WOODHOUSE G. W. (1983) A geochemical reconstruction of oil generation in the Barrow Sub-basin of Western Australia. *Geochim. Cosmochim. Acta* **47,** 2091–2105.

WHITEHEAD W. L. (1954) Hydrocarbons formed by the effects of radioactivity and their role in the origin of petroleum. In *Nuclear Geology* (ed., H. FAUL), pp. 195–218. J. Wiley & Sons.

WIESE R. G., JR. (1973) Mineralogy and geochemistry of the parting shale, White Pine, Michigan. *Econ. Geol.* **68,** 317–331.

WRONKIEWICZ D. J. and CONDIE K. C. (1987) Geochemistry of Archean shales from the Witwatersrand Supergroup, South Africa: Source area weathering and provenance. *Geochim. Cosmochim. Acta* **51,** 2401–2416.

## APPENDIX I: RADIOGENETIC HEAT CALCULATIONS

The overall heat generated by radioactive decay of one gram of uranium in a year has been determined by BIRCH (1954) to be 0.73 cal, which may be expressed as $9.685 \cdot 10^{-2}\ \mu Wg^{-1}$. Using this value for a rock with a density of 2.2 $Mgm^{-3}$ and a uranium concentration of 440 ppm gives a radiogenic heat value of 93.75 $\mu Wm^{-3}$. A 10-meter thick Alum Shale of this composition has a radiogenic heat flow of 937.5 $\mu Wm^{-2}$. Addition of this radiogenic heat flow to a mean global heat flow of 62.7 $mWm^{-2}$ (LEE, 1963) gives a composite heat flow of 63.6 $mWm^{-2}$. A mean measured thermal conductivity of 1.69 $Wm^{-1}\ K^{-1}$ for the Alum Shale (KRISTIANSEN *et al.*, 1982) results in calculated thermal gradients inclusive and exclusive of radiogenic heat of 37.6°C $Km^{-1}$ and 37.1°C $Km^{-1}$, respectively. This indicates that radiogenic heat from a 10-meter thick Alum Shale with a 440 ppm uranium content increases the thermal gradient by only 1.3 percent.

## APPENDIX II: DERIVATION OF EQUATION 1

The sums of available decay energies for the overall decay of $^{238}U$ and $^{235}U$ are 47.4 and 45.2 MeV, respectively (BIRCH, 1954). Therefore, the total available energy ($Q$) emitted from decaying uranium in 100 g of rock is expressed as

$$Q = 47.4N_{238} + 45.2N_{235} \quad \text{(A1)}$$

where $N$ is the number of uranium atoms (*i.e.*, $^{238}U$ and $^{235}U$) in 100 g of rock that have completely decayed over a specified time interval, $\Delta t$. The first-order rate law for the decay of both uranium isotopes may be expressed as

$$U_o = \frac{U_t}{e^{-\lambda \Delta t}} \quad \text{(A2)}$$

where $U_o$ is original concentration of uranium, $U_t$ is concentration of uranium at the end of a specified time interval ($\Delta t$), and $\lambda$ is the decay constants. Using the decay constants from JAFFEY *et al.* (1971), Eqn. (A2) becomes

$$^{238}U_o = \frac{^{238}U_t}{e^{-1.55\times10^{-10}\Delta t}} \quad \text{and} \quad ^{235}U_o = \frac{^{235}U_t}{e^{-9.8485\times10^{-10}\Delta t}}. \qquad \text{(A3 and A4)}$$

Assuming $^{238}U_t$ and $^{235}U_t$ may be equated to present-day relative abundances (0.992743 for $^{238}U$ and 0.00720 for $^{235}U$; FAURE, 1986, p. 284), their concentrations may each be expressed as a percentage of the total present-day uranium concentration, $\bar{U}_t$;

$$^{238}U_t = 0.992743\bar{U}_t \quad \text{and} \quad ^{235}U_t = 0.00720\bar{U}_t. \qquad \text{(A5 and A6)}$$

Substituting Eqns. (A5) and (A6), respectively into Eqns. (A3) and (A4), and subtracting Eqns. (A5) and (A6) from the resulting expression gives

$$^{238}U_o - ^{238}U_t = \frac{0.992743\bar{U}_t}{e^{-1.55\times10^{-10}\Delta t}} - 0.992743\bar{U}_t \qquad \text{(A7)}$$

and

$$^{235}U_o - ^{235}U_t = \frac{0.0072\bar{U}_t}{e^{-9.8485\times10^{-10}\Delta t}} - 0.0072\bar{U}_t. \qquad \text{(A8)}$$

The number of uranium atoms that have completely decayed (N) within the time interval $\Delta t$ is calculated by dividing Eqns. (A7) and (A8) by the molecular weight of their uranium isotopes and multiplying the quotient by Avogadro's number. The resulting expressions are substituted into Eqn. (A1), which simplifies to Eqn. (1);

$$Q = \bar{U}_t\left[\frac{1.1905\times10^{23}}{e^{-1.55\times10^{-10}\Delta t}} + \frac{8.3304\times10^{20}}{e^{-9.8485\times10^{-10}\Delta t}} - 1.1988\times10^{23}\right].$$